Direct and sensitised photolysis of dispersed photoacid generators to formulate water-borne photopolymers†

Kunihiro Ichimura*[ab]

Received 10th October 2006, Accepted 21st November 2006
First published as an Advance Article on the web 11th December 2006
DOI: 10.1039/b614744c

Casting a photopolymer solution to form a film, followed by image-wise photoirradiation and subsequent wet development, leads to photolithography. Whereas the wet development is achievable with aqueous alkali, the emission of an organic solvent as a volatile organic compound (VOC) is usually inevitable during the film casting because ingredients of common photopolymers are insoluble in water. This work proposes water-borne photopolymers cast and developed solely with neutral water by incorporating mechanically milled sub-micron particles of poorly water-soluble photoacid generators (PAGs), which undergo direct and sensitised solid-state photolysis to make a poly(vinyl alcohol) film insoluble in water with the aid of acid-sensitive crosslinkers. The sensitised solid-state photolysis of onium-type PAGs in the solid state was studied in detail to extend the spectral sensitivity of this kind of photopolymer. Fluorescence quenching measurements revealed that the solid-state sensitisation occurs through singlet exciton migration in sensitiser particles followed by electron transfer to PAG particles at the solid–solid boundary region. Three-component photopolymers comprised of an aqueous dispersion of PAG in the absence or in the presence of a co-milled sensitiser, poly(vinyl alcohol) and a water-soluble diepoxy were formulated to display photosensitivity of 17 mJ cm^{-2} by the direct photolysis of a dispersed sulfonium salt and that of *ca.* 120 mJ cm^{-2}, for instance, by the photolysis of an iodonium salt sensitised with co-milled 9,10-dipropoxyanthracene.

Introduction

Photolithographic processes consist of spreading a photopolymer solution to fabricate a thin film on a substrate, followed by image-wise exposure and wet development to remove unexposed or exposed areas selectively to give negative-type or positive-type relief patterns. Photolithography without using any organic solvent has been urgently desirable to carry out non-VOC (volatile organic compound) processes not only for large-scale production of micron-scale relief images applicable to dry film resists, solder resists, photopolymers for printing plates and so forth,[1] but also for sub-micron or nano-patterning in semiconductor industries.[2] But there have been only a few photopolymers processed solely with neutral water as a safe and readily available solvent. Except for classical water-developable photopolymers cross-linked by means of dichromate salts, diazo resins and water-soluble diazides, commercially available water-developable photopolymers are poly(vinyl alcohol) (PVA) substituted with photodimerisable styrylpyridinium side chains in anomalously low loadings.[1,3] They have been used not only for making printing plates and the other photolithographic applications, but also for immobilizing bioactive substances including enzymes, microbial cells and so forth.[1] The other photocross-linkable polymers cast and developed with water have been prepared by tethering aromatic azide moieties to water-soluble polymers to improve photosensitivity.[4] These types of photopolymers become water-insoluble solely photochemically. Accordingly, a level of crosslinking density is specifically determined by loading of photosensitive moieties, leading sometimes to problems arising from swelling of crosslinked films in water. On the other hand, chemistries for widely spread photopolymers including the following two types involve not only photochemical events, but also subsequent thermal reactions. The first is predominantly based on the deprotection of side chains or crosslinking of backbone polymers catalysed by photogenerated acids.[5] The second is based on photoinduced radical or cationic polymerisations of monomers[6] mixed physically with, or covalently tethered to, backbone polymers. Chemically amplified photoresists (CAP) are based on the first class, and efforts have been made on exploiting negative- as well as positive-type CAP processed with water.[2,7] Water-soluble PAGs were developed for this purpose. The second chemistry involving photopolymerisation usually requires a radical photoinitiator or PAG dissolved in fluid or solid. Though wet development is attainable by using an aqueous alkali for these types of photopolymers, the emission of organic solvents is inevitable during the film casting. This is because conventional photoinitiators or PAGs are hardly soluble or insoluble in water so they are dissolved in

[a]*Faculty of Science, Toho University, 2-2-1 Miyama, Funabashi, Chiba 274-8510, Japan. E-mail: k-ichimura@sci.toho-u.ac.jp; Fax: +81-47-472-1331; Tel: +81-47-472-1331*
[b]*Research Centre for Materials with Integrated Properties, Toho University, 2-2-1 Miyama, Funabashi, Chiba 274-8510, Japan*

† Electronic supplementary information (ESI) available: Tables of the effect of milling period on particle size, milling formulation and the dependence of photosensitivity on preparative methods; Stern–Volmer plots for **3a** in solution and in dispersion, photosensitive curves for **8** and **9** as crosslinkers and of type-C photopolymers containing milled mixtures of **2a** and **3a**. See DOI: 10.1039/b614744e

This journal is © The Royal Society of Chemistry 2007

organic solvents to combine with polymers bearing carboxylic residues to formulate homogeneous solutions. Huge amounts of radical as well as cationic or even hybrid polymerisation-type photopolymers are used in industries for micron-scale photolithography because of good availability of components and flexible materials design for versatile applications. In this context, a way of approaching polymerisation-type water-borne photopolymers realizing non-VOC processes is strongly required. One of the approaches is based on improving the water-solubility of photoinitiators[8] or PAGs,[7] whereas numerous patent literatures are available concerning emulsifying hydrophobic monomers dissolving a radical photoinitiator in water to devise water-borne photopolymers.

Our strategy to formulate water-borne photopolymers is based on dispersing hardly water-soluble or water-insoluble PAGs as nano-sized particles in water to make films, which are developable with water after photopatterning. Taking into consideration that readily available PAGs are sensitive to wavelengths far shorter than *ca.* 350 nm, the expansion of their spectral sensitivity to be matched with conventional light sources should be considered from a practical viewpoint. In this respect, the solid-state sensitisation of PAGs is needed. Whereas elegant ways are reported to sensitise onium-type PAGs intramolecularly by binding a sensitiser moiety to a PAG molecule covalently[9] or by salt formation[10] to improve electron transfer efficiencies, the author's interest headed for examining solid-state electron transfer from a sensitiser to a PAG. This is simply because no chemical modification for modulating the solubility of both may be needed in solid-state photochemistry so that commercially available PAGs can be employed as received. In this context, aqueous dispersions of organic solid particles in the size range of nanometre to sub-micrometre[11] are very fascinating because of pseudo-solution behaviour exhibiting high transparency as a result of notable suppression of light scattering. Concerning solid-state electron transfer, there had been no report, to the author's knowledge, except for hole injection from a dye layer[12] or a solute such as tetrachlorophthalodinitrile[13] into anthracene crystals to induce photocurrent. But the following facts motivated the author to do with the solid-state photosensitisation. Since the first report by Bowen,[14] energy transfer systems in organic solids have been extensively studied[15] in relation to organic light emitting diodes[16] and photovoltaic solar cells[17] to reveal that intermolecular photophysical processes take place through exciton diffusion in crystals. This situation means that the distance between donor and acceptor molecules for electron transfer can be much elongated by means of exciton diffusion.

This work aims to verify the validity of formulating cationic water-borne photopolymers by using aqueous dispersions of PAGs and mixtures of PAGs and sensitisers to achieve solid-state photoacid generation.[18] The brief description of preparing nano-sized crystalline particles by mechanical milling is followed by studies on photochemical events of aqueous dispersions of PAGs co-milled with sensitisers to elucidate solid-state photosensitisation through crystal-to-crystal electron transfer liberating photoacids. Acidic species generated by the direct and sensitised photoacid generation work as an initiator or a catalyst for crosslinking of PVA with the aid of water-soluble acid-sensitive crosslinkers to demonstrate photolithography treated exclusively with neutral water throughout the process.

Experimental

Materials

Materials used in this study are shown in Fig. 1. The sulfonium (**1**) and iodonium salts (**2a**) were gifted by San-Apro and Midori Kagaku, respectively, whereas the triflate (**2b**) and chloride (**2c**) were purchased from Sanwa Chemical and Tokyo Kasei, respectively. Dialkoxyanthracenes (**3a** and **3b**), the thioxanthone (**4**) and the ketocoumarin (**5**) were donated by Kawasaki Kasei Chemicals, Nippon Kayaku and Midori Kagaku, respectively. Anthracene (**3c**) (zone-refined), diphenylanthracene (**3d**), perylene (**6**) and pyrene (sublimed) were purchased from Aldrich. The hexamethylolmelamine (**7**) and diepoxy (**8**) were donated by Sanwa Chemical and Nagase Chemtex, respectively. They were all used without further purification.

Physical measurements

Particle size distributions were taken on a Nano-Z, Sysmex, whereas absorption and fluorescence spectra were taken on a diode array Multistep 1500 and an RF-5300PC of Shimadzu, respectively. Film thickness was recorded on a profilometer (Tencor, Alpha-Step IQ) to obtain photosensitivity curves.

Fluorescence measurements were performed as follows. A dilute dispersion of **3a** of OD = *ca.* 0.15 at λ_{max} = 391 nm was placed in a quartz cell to record a fluorescence spectrum at a conventional 90° geometry to perform quenching experiments by water-soluble **2c**. The fluorescence measurement of a concentrated (*ca.* 1 wt%) dispersion of a sensitiser was performed by setting it in a quartz cell of 3 mm depth to be excited at a 45° incidence to capture the emission from a surface layer at a 90° geometry. Care was taken to record quenched emission spectra in the presence of co-milled **2a** quickly in a narrow wavelength region of 30 nm centered at the emission band at 465 nm for **3a** to minimise the effect of reducing fluorescence intensity during the excitation owing to the solid-state photosensitised conversion. Combinations of **2a**

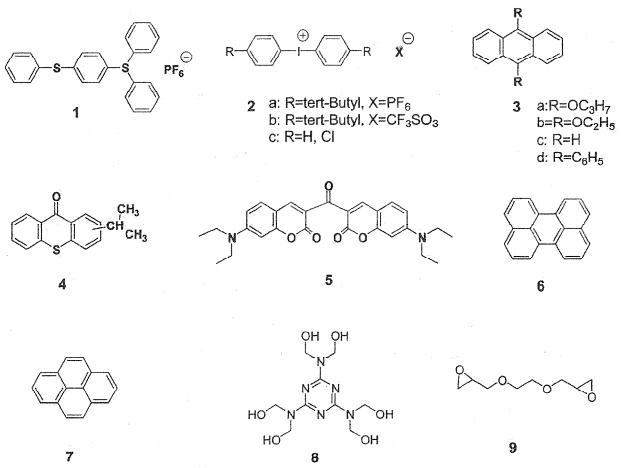

Fig. 1 Molecules employed in this study.

This journal is © The Royal Society of Chemistry 2007

with the other sensitisers were subjected to fluorescence quenching measurements in a similar way. The excitation of **3a** and **3b**, **3c**, **3d**, **6** and **7** were achieved at 391, 391, 374, 380 and 370 nm, respectively.

Wet milling of a mixture of 2a and 3a as a typical procedure

An aqueous 5 wt% solution of PVA (DP = 500) (9.59 g) was placed in a grinding bowl (volume = 45 mL) made of zirconia containing zirconia beads of 3 mm diameter (10 mL), followed by adding 302.2 mg of crystals of **2a** and 110.8 mg of **3a** in a 1 : 1 molar ratio to be subjected to grinding at 400 rpm for 1 h in the presence of a few drops of an anti-foaming agent by using a planetary mill (Fritsch; Pulverisette 7). An averaged particle size of a dispersion thus prepared was 850 nm with a polydispersity index (PDI) of 0.459. Subsequently, the milling media was replaced by zirconia beads of 0.3 mm diameter to grind at 650 rpm for 1 h, followed by removing the beads by filtration to give particles of a size of 342 nm with a PDI of 0.214. Zirconia beads of diameters of 0.1 mm and 0.05 mm were also used if necessary.

Photoirradiation

A dilute aqueous dispersion of PAGs or a mixture of PAGs and a sensitiser was exposed to >350 nm light from a 500 W super-high pressure mercury arc and subjected to UV spectral measurements at intervals to follow the reaction. Preparative photochemistry of a dispersion of **3a** was performed by irradiating an aqueous 0.2 wt% dispersion (20 mL) with >350 nm light until characteristic absorption bands of the anthracene disappeared completely. The dispersion was extracted with ethyl acetate, and the organic layer was washed with water, followed by drying over magnesium sulfate and evaporating the solvent to isolate anthraquinone. A 70% yield of the product was estimated by UV spectral measurement of the organic layer.

An aqueous dispersion (0.2 wt%) of a mixture of PAGs and a sensitiser (20 mL) was exposed to >350 nm light from the mercury arc and subjected to alkaline titration with an 8.50×10^{-3} M NaOH solution using phenolphthalein as a colour indicator to estimate the amount of acid generated.

Photosensitivity determination

A suspension of 500.0 mg of the sulfonium salt (**1**) in 9.50 g of a 5 wt% of PVA (DP = 500) was ground in the planetary mill with zirconia beads of 0.3 mm diameter at 650 rpm for 2 h. A milky-white dispersion (1.00 g) was mixed thoroughly with 2.00 g of a 10 wt% aqueous solution of PVA (DP = 1700), 32.0 mg of the epoxy (**4**) and 0.5 g of deionised water to formulate a photosensitive composition. The dispersion was spin-cast on a glass plate at 1000 rpm, followed by blowing with a hair drier warmly to form a dried thin film, which was exposed to 313 nm light from a Hg–Xe lamp (SAN-EI Electric Co.; UVF-203S) passed through a solution filter (K_2CrO_4) and a glass filter (Asahi Technogalss; UV-D35). The film was baked at 110 °C for 2 min and developed with neutral water to record the remaining film thickness to obtain a photosensitivity curve. Photosensitivity curves for the other photopolymers were obtained in a similar fashion after exposure to 365 nm light (filters; UV-35 and UV-D35) or >350 nm (a filter; UV-35) light.

Results and discussion

Approaching non-VOC photolithographic processes based on the present concept, there are three steps to be exploited. The first is to achieve the nano-downsizing of crystalline particles of water-insoluble PAGs and mixtures of PAGs and a sensitiser to reduce light scattering of their dispersions, leading to improved optical quality of photosensitive films. Bead milling was employed here because of the ready availability of a tabletop planetary mill to carry out small-scale experiments. The second is to corroborate the photoacid generation from PAG sub-micron particles thus prepared. In this context, photochemistry of aqueous dispersions of sensitisers and mixtures of PAGs and sensitisers should be elucidated. The third is to apply the solid-state photoacid generation to water-developable photopolymer systems by employing a water-soluble polymer and an acid-sensitive crosslinker.

Preparation of aqueous dispersions of PAGs

First of all, water-solubility of the PAGs and sensitisers employed in this study (Fig. 1) is mentioned here in regard to the mechanism of solid-state sensitisation discussed below. Crystals of a sample were suspended in water under shaking to record an absorbance at λ_{max} of a filtrate after removing the solid by paper filtration to estimate a saturated concentration. As summarised in Table 1, water-solubility of the onium-type PAGs (**1**, **2**) was influenced, in particular, by a counteranion. Aromatic sensitisers (**3**, **4**, **6** and **7**) were essentially insoluble in water, whereas the ketocoumarin (**5**) was slightly water-soluble.

Nano-sized organic crystals have been so far fabricated by a reprecipitation technique consisting of pouring a dilute solution of an organic compound in a good solvent into a poor solvent under stirring,[19] if necessary under ultrasonication,[20] or microwave irradiation,[21] to give nano-dispersions. An alternative way has been reported to give aqueous nano-dispersions of organic crystals by the layer-by-layer vacuum deposition of water and organic molecules on a cooled substrate plate in vacuum.[22] Since conventional PAGs are of onium salts, the latter method is not suitable to the present purpose. Therefore, the reprecipitation method was at first examined to prepare aqueous dispersions of **3a** as a sensitiser and the iodonium hexafluorophosphate (**2a**) as a PAG. According to the literature, a dilute (1×10^{-3} wt%) acetone solution of **3a** was added carefully into water under stirring. Whereas a slightly turbid dispersion was obtained at the early stage of the addition, the deposition of crystals occurred

Table 1 Solubility of onium-type PAGs in water

PAG	Saturated conc./mol L^{-1}	λ_{max} in water/nm
1	9.2×10^{-5}	302
2a	4.6×10^{-4}	239
2b	1.1×10^{-3}	239
2c	8.3×10^{-2}	227

This journal is © The Royal Society of Chemistry 2007

suddenly at a critical volume of the solution. Quite the same situation was observed for **2a** and a 1 : 1 (mol : mol) mixture of **2a** and **3a**. Whereas aqueous dispersions of nano-particles with averaged sizes ranging from 200 nm to 300 nm were prepared under specified conditions, this method was unsuitable for the present work, because the concentration of dispersed particles was too low ($<1 \times 10^{-4}$ wt%) to formulate photosensitive polymers doped with PAGs, concentrations of which should be few wt% or more.

Accordingly, we carried out bead milling by using a tabletop planetary mill to grind PAG crystals with or without the sensitiser in an aqueous solution of PVA in the presence of an anti-foaming agent. PVA was used as both a dispersion stabiliser and a binder polymer to be crosslinked acid-catalytically. Averaged particle sizes were influenced not only by grinding speed and period, but also by the nature of the components. A typical example of the effect of milling period on particle size is shown in Table S1.[23] The results revealed that 3 h milling gives the optimal result in this case whereas particles begin to grow upon further mechanical treatment. It followed that appropriate conditions were optimised for each sample to obtain milky-white dispersions containing particles of sizes of sensitisers and mixtures of sensitisers and PAGs in the range from *ca.* 200 nm to 500 nm. The results are summarised in Table S2.[23]

Photochemistry of dispersed sensitisers

9,9′-Dialkoxyanthracenes[24] and thioxanthones[25] sensitise the photolysis of iodonium and sulfonium salts effectively to liberate strong acids. The photofatigue of **3a** and **4** dispersed in water in the absence of PAGs was monitored by tracing spectral changes during UV irradiation prior to examining the photochemistry of dispersed mixtures of a sensitiser and PAG. It was found unexpectedly that **3a** dispersed in water disappears upon >350 nm light irradiation and the solid-state degradation proceeds rather faster than in a hexane solution. As shown in Fig. 2A, the photoirradiation resulted in a decrease in the characteristic absorption bands of wavelengths longer than *ca.* 350 nm ascribable to the anthracene moiety to generate a new band centred at *ca.* 335 nm. Preparative photochemistry revealed that anthraquinone (AQ) is formed in good yield as a photoproduct. The solid-state photochemistry was confirmed by exposing crystals of **3a** or **3d** to UV light. Intensely fluorescent crystals displayed colour changes from

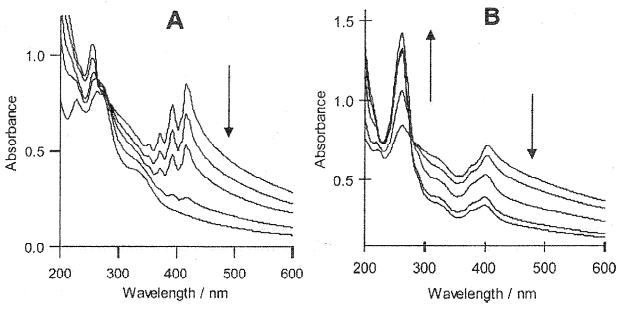

Fig. 2 Spectral changes of (A) **3a** and (B) **4** dispersed in an aqueous solution of PVA upon exposure to >350 nm light for 0, 20, 60, 120 and 240 sec and for 0, 6, 25, 36 and 44 min, respectively.

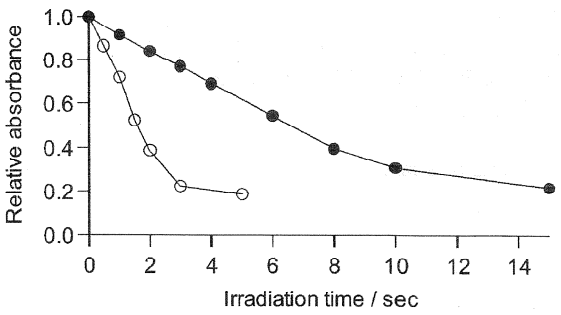

Fig. 3 UV photolysis of **3a** dispersed in water under aerobic (●) and anaerobic (○) conditions.

yellowish into brown together with reduction of fluorescence intensity. Note here that it is advisable to avoid exposure of this type of sensitiser solid even to ambient light. In order to obtain further information of the solid-state formation of AQ, irradiation was carried out under argon stream to know whether photooxygenation participates in the photoreaction. Contrary to our anticipation, the photodegradation was accelerated rather under anaerobic conditions, as shown in Fig. 3. This situation indicates that oxygen quenches the photoreaction and that the (4 + 2) photocycloaddition of the oxygen molecule to the anthracene moiety plays no role in the formation of AQ. It follows that the solid-state photoconversion accompanied by two-electron oxidation may be illustrated as shown in Fig. 4. An excited molecule of **3** is coupled with a nearest neighbour molecule in a crystal to form an excimer, which undergoes charge separation to form a couple of a radical cation and an anion. An alkyl radical is eliminated from the radical anion to give an anionic species, which transfers one electron to the radical cation to give AQ and to regenerate the starting molecule.

UV exposure of **4** also led to marked spectral alteration, as sketched in Fig. 2B. Note, however, that the positions of λ_{max} of characteristic absorption bands are essentially not altered even after prolonged irradiation although spectral shapes are considerably modified. This means that no change in molecular structure occurs. In fact, **4** was recovered by extraction from a UV-exposed dispersion with ethyl acetate. Since these results implied that the spectral changes of the dispersion come from physical properties of particles of **4**, changes in particle

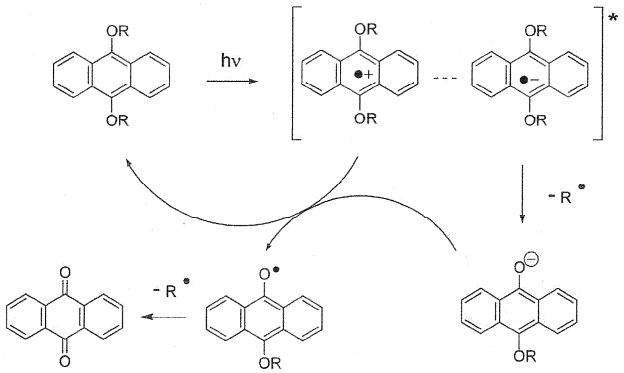

Fig. 4 Proposed mechanism for the solid-state photoconversion of 9,9′dialkoxyanthracene (**3**) into anthraquinone.

size distribution were monitored by dynamic light scattering (DLS) during UV irradiation. It was observed that an averaged particle size of 898 nm before UV irradiation is reduced monotonously down to 488 nm upon prolonged irradiation. Though further study is necessary, it is very likely that UV irradiation leads to the break of crystalline particles of **4** without a chemical reaction. Photoinduced size reduction was observed also for an aqueous dispersion of **3a** from 368 nm to 183 nm. In this case, the crystal break is likely to be triggered by the AQ formation. It should be noted that this sort of photoinduced size reduction of crystalline particles makes a turbid dispersion more transparent, leading to improving optical quality of a dispersed solution and film by photoirradiation.

Photochemistry of mixtures of sensitisers and PAGs

Photochemistry of aqueous dispersions of **2a** and co-milled sensitisers was examined preliminarily by spectral measurements. The photoinduced disappearance of **3a** in dispersions was accelerated by co-milling with an equimolar amount of **2a** crystals (Fig. S1A),[23] when compared with the result in the absence of **2a** (Fig. 2A). The photospeed was enhanced markedly when the molar ratio was **3a** : **2a** = 1 : 3. UV-exposed aqueous dispersions of **2a** and **3a** mixtures became acidic after thorough disappearance of absorption bands of **3a**. Their absorption spectra displayed λ_{max} centred at *ca.* 335 nm ascribable to AQ, indicating that the sensitised photolysis of **2a** occurs even in solid-state dispersions and competes with the formation of AQ. Photoirradiation of a dispersion of **2a** with co-milled **5** displayed also the disappearance of the band at λ_{max} = *ca.* 240 nm due to **2a** (Fig. S1B).[23] All of the results imply the occurrence of sensitised photolysis.

Attempts were made to follow the photoacid generation during UV irradiation of the dispersions by means of tetrabromophenolphthalene tetrasulfonate as a colour indicator. But this convenient method was not applicable to the present system. The iodonium cation combined with the sulfonate units of the dye to form a complex soluble in an organic solvent such as acetone, leading to severe modification of spectral shape. Consequently, alkaline titration was carried out. But an end point of the titration was not clear for the **2a**-sensitiser system, and yields of acidic species estimated exceeded theoretical ones. This is probably because of a ligand exchange of HPF_6 with H_2O to generate HF.[26] In this context, the triflate salt (**2b**) was employed for determining photoacid generation by alkaline titration on account of the stability of the anion toward alkali. It should be mentioned here that longer exposure time was needed, implying lower reactivity of **2b** when compared with **2a**. As shown in Fig. 5A, approximately quantitative generation of the acid was observed for a 1 : 1 (mol : mol) mixture of **2b** and **3a** under exclusive excitation of **3a** (open squares in Fig. 5A). On the other hand, the chemical yield of photoacid levelled off at *ca.* 50% with respect to **2b** when the mixing ratio of **2b** and **3a** is 0.5 : 1 (open triangles in Fig. 5A). It was assumed that the lower loading of **2b** allows the predominant occurrence of the side reaction to give AQ. In line with this assumption, a 3 : 1 (mol : mol) mixture generates a photoacid in a yield of 231% on the basis

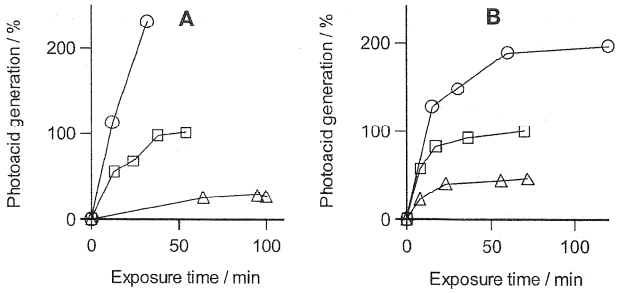

Fig. 5 Chemical yields of a photogenerated acid from **2b** dispersed in water in the presence of (A) co-milled solids of **3a** in mixing ratios (mol : mol) of 1 : 0.5 (△), 1 : 1 (□) and 1 : 3 (○) and (B) co-milled solids of **4** in mixing ratios (mol : mol) of 1 : 0.5 (△), 1 : 1 (□) and 1 : 2 (○) upon exposure to >350 nm light, respectively.

of **3a** loading (open circles in Fig. 5A), which is equivalent to the relatively high yield of 77% with respect to **2b**, suggesting that **3a** works as a sensitiser sufficiently. The photoacid generation sensitised with **4** is shown in Fig. 5B. Almost quantitative photoacid generation was observed for every mixing ratio. This is in accord with the photofatigue resistance of **4** in the absence of PAG. Fig. 6 summarises the photoacid generation from **2b** sensitised with various sensitisers including **3c**, **3d** and **6** co-milled in a 1 : 1 (mol : mol) ratio. **3a** and **4** act as the best sensitisers among them, followed by **3c**, whereas sensitisation efficiencies of **3d** and **6** were far lower. Concerning the ketocoumarin (**5**), it was difficult to trace the photosensitised acid generation by the alkaline titration using phenolphthalein because of the intense colour of **7**.

All of the results described above mean that the photoacid generation comes from solid-state electron transfer from a sensitiser to **2b**. Note here, however, that the salt is ionic so the water-solubility of 1.1×10^{-3} M cannot be neglected in this system. In order to check the possibility of whether the electron transfer occurs from excited sensitiser solid to photoacid generator molecules dissolved in water, diphenyliodonium chloride (**2c**) as a more water-soluble PAG was employed to prepare aqueous solutions to be mixed with an aqueous dispersion of **3a**. A photodegradation rate of **3a** was essentially not influenced by the presence of **2c** at a concentration of 2×10^{-3} M. It can be concluded that soluble

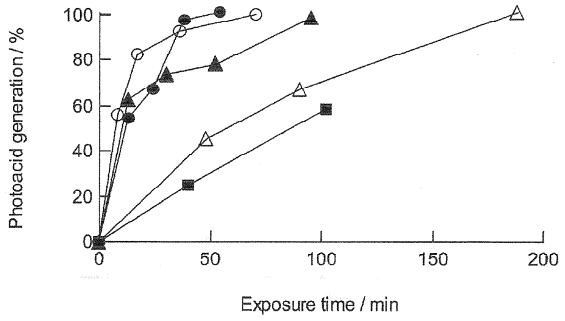

Fig. 6 Chemical yields of a photogenerated acid from PAG (**2b**) dispersed in water in the presence of an equimolar amount of co-milled solids of **3a** (●), **4** (○), **3c** (▲), **6** (△) and **3d** (■), respectively, upon exposure to >350 nm light.

This journal is © The Royal Society of Chemistry 2007

fractions of **2b** play a negligible role in the photoacid generation.

Fluorescence measurements

To the author's knowledge, there has been no report on solid-state sensitised photochemistry through electron transfer among organic crystals except for hole injection to achieve photocurrent measurements.[12,13] In this context, it was checked first whether electron transfer from **3a** to an iodonium salt at the solid–fluid interface is possible. The chloride (**2c**), which is fairly water-soluble (Table 1), was used for fluorescence quenching experiments. Note again that **3a** is not soluble at all as revealed by particle size analysis and absorption spectral measurements exhibiting a marked red shift and broadening of absorption bands in a dilute dispersion (Fig. S2).[23] A Stern–Volmer constant ($k_q\tau$) in water was 8.6, whereas $k_q\tau$ in acetonitrile solutions was 119 (Fig. S3).[23] The results reveal the following. The fluorescence quenching of **3a** particles by soluble **2c** can occur at a solid–water interface. But assuming that a quenching constant (k_q) of **2a** is not far from that of **2c**, a level of fluorescence quenching by a soluble fraction of **2a** of 1.1×10^{-3} M is estimated to be 0.2% and negligibly small. This draws the conclusion that **2a** can act essentially as a solid-state fluorescence quencher.

Fluorescence measurements of **3a** co-milled with **2a** to evaluate solid-state quenching efficiencies were achieved by using aqueous dispersions containing 1 wt% of **3a** under excitation at a 45° incidence with respect to the cell surface to capture the emission from a surface layer at a 90° geometry. This is because estimating accurate absorbances at the excitation wavelength of dilute dispersions was difficult due to light scattering so the conventional 90° geometry measurement was not suitable. As illustrated in Fig. 7, since the spectral shapes of fluorescence of the 1 wt% dispersions in shorter wavelength regions were modified due to the internal filter effect, quenching was monitored at the third peak centered at 465 nm. Furthermore, measurements were conducted quickly, since emission intensity was reduced during the excitation owing to the solid-state photosensitised conversion. Fig. 8A shows relative fluorescence intensity (Φ/Φ_0) as a function of molar fractions of co-milled **2a** (open circles). Φ and Φ_0 denote the fluorescence intensity of **3a** without and with co-milled **2a**, respectively. The results disclose that the

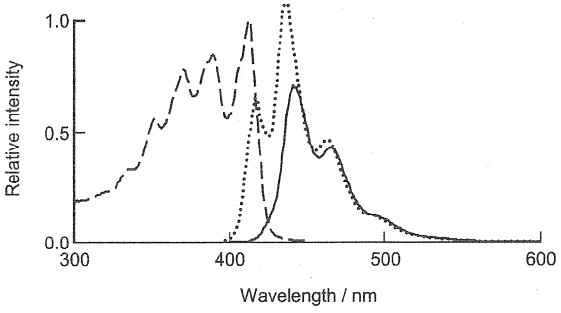

Fig. 7 Fluorescence spectra of **3a** in a dilute aqueous dispersion (dotted line) and in a 1 wt% dispersion (solid line) and excitation spectrum of the dilute dispersion (broken line).

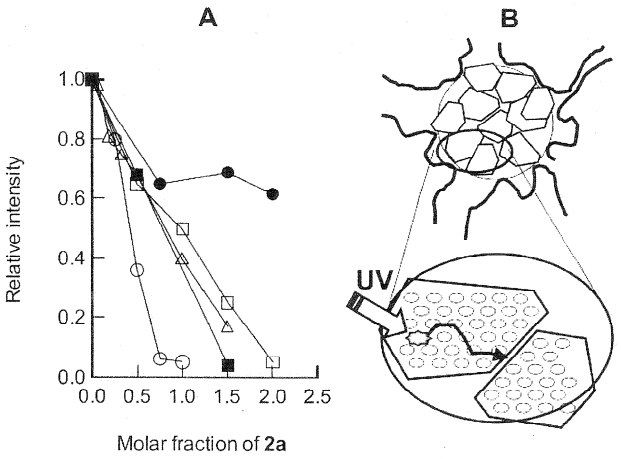

Fig. 8 Solid-state fluorescence quenching in an aqueous dispersion. (A) Fluorescence intensities of particles of **3a** (□), **3b** (△), **3c** (○), **3d** (●) and **7** (■) dispersed in water as a function of weight ratios of co-milled **2a**. (B) The illustrative representation of the sub-particle/exciton model for crystal-to-crystal fluorescence quenching, whereas DLS measurement detects a particle surrounded by PVA chains, which is shown as a gray circle.

fluorescence decreases linearly with an increase of the molar ratio of the solid quencher. In order to reveal a general aspect of crystal-to-crystal fluorescence quenching by **2a**, aqueous dispersions of fluorescent crystals of anthracene (**3c**), its derivatives (**3b** and **3d**) and pyrene (**7**) were co-milled with **2a** at various mixing ratios. **3a**, **3c**, **3d** and **7** exhibited linear decreases of fluorescence intensity as a function of the loading of **2a** in a way similar to **3a**. On the other hand, it should be noteworthy that the fluorescence quenching of **3d** levels off at about 30–40% (full circles) and that no further quenching occurs even in the presence of excess amounts of **2a**.

It is very probable that the photoinduced solid-state electron transfer takes place specifically between donor and acceptor molecules exposed to the topmost surfaces of grains. Accordingly, the diffusion of singlet excitons in sensitiser crystals[15] plays an essential role to convey excited energy to a surface donor molecule, which transfers an electron to a surface acceptor molecule through the grain boundary. First of all, discussion is made on the combination of **3c** and **2a**, because **3c** has been one of the most extensively studied compounds for exciton diffusion. The diffusion length (DL) of singlet excitons in crystals of **3c** has been reported to be in the range of 46 nm to 77 nm[15,22,27] so that the fluorescence can be sufficiently quenched when the averaged radius (Rs) of particles is shorter than DL. The fact that the fluorescence of milled **3c** particles is thoroughly quenched even though a particle size (= 2 Rs) of *ca.* 300 nm is much larger than the DL value can be reasonably interpreted in terms of the following assumptions. First, size distributions analysed by DLS correspond not to primary particles, but to aggregated or agglomerated sub-grains of milled **3c**. Second, the agglomerated or aggregated particles consist not only of sub-grains of **3c**, but also of those of **2a**. Thirdly, solid-state electron transfer occurs among the sub-grains as a result of intimate contact of **3c** with **2a**. This situation is sketched in Fig. 8B.

This journal is © The Royal Society of Chemistry 2007

Consequently, if Rs of sub-grains of a sensitiser solid is shorter than DL, fluorescence quenching occurs sufficiently as a result of direct contact among sub-grains of the sensitiser and **2a**. This is the case for the **3c**–**2a** combination. The requirement of higher loadings of **2a** for thorough fluorescence quenching of **3a**, **3b** and **7**, when compared with **3c**, may arise from the difference in DL values, which may be shorter than those of **3c**, whereas the DL values are not available. The solid-state fluorescence quenching behaviour of **3d** is also in line with the assumptions. DL of **3d** was reported to be 5.5 nm[28] and much shorter than that of **3c**. It is very likely that Rs of sub-grains of **3d** is far shorter than DL under the present milling conditions so that the quenching occurs only at the surface region of the sub-grains, leading to insufficient quenching efficiencies, which level off even in the presence of excess amounts of **2a**. As shown below, the fluorescence quenching behaviour is in accord with quite low photosensitivity of the type-C photopolymer dispersing the **2a**–**3d** combination. Poor photosensitisation efficiency of perylene (**6**) arises also from a short DL, which was reported to be 0.34 nm.[22] Concerning non-fluorescent or weakly fluorescent sensitisers for **2a**, it is known that electron transfer from thioxanthone (**5**)[25] and ketocoumarin (**7**)[29] takes place from their triplet state. The diffusion of triplet excitons[15b] in these types of sensitiser crystals plays an essential role in solid-state photosensitisation.

PAG-dispersed photopolymers

In order to verify the validity of our concept of PAG-dispersed photopolymer systems, an aqueous dispersion of the sulfonium salt (**1**) was employed for the photoacid generation at first. This is because the monomolecular photolysis of the PAGs occurs even in the solid-state.[30] PVA of DP = 1700 was used as a binder polymer, and its aqueous solution was mixed with an aqueous dispersion of **1**. Two kinds of water-soluble acid-sensitive crosslinkers, a methylolmelamine derivative (**8**)[7b] and a diepoxy compound (**9**), were added to the mixture, respectively, to examine photosensitivity characteristics. This type-A photopolymer was comprised of **1**, PVA and a crosslinker in concentrations of 0.60, 6.0 and 1.00 wt%, respectively. A spin-cast thin film was exposed to UV light, followed by post-exposure baking to accelerate the acid-catalysed crosslinking of PVA chains and development with water. It was revealed that difunctional **9** is better even though **8** is multifunctional (Fig. S4).[23] The superior performance of **9** may come from the contribution of ring opening cationic polymerisation, which competes with the addition to OH residues of PVA main chains. On the basis of these results, **9** was used for the subsequent photosensitivity determination. It is known that conversions of epoxides in their UV cationic curing are reduced by high relative humidity.[31] In this context, there is the possibility that residual water in films may influence photosensitivity characteristics more or less due to the hydrophilicity of PVA and the film preparation from aqueous solutions. Though the optimisation of conditions including prebaking is necessary, spin-cast films were dried in this work by blowing with a hair drier warmly and subjected to photosensitivity determination.

As shown in Fig. 9, thorough insolubilisation with a high contrast ratio was observed at an exposure dose of about 17 mJ cm^{-2} (closed circles), exhibiting photosensitivity comparable to conventional photopolymers. Taking quite a low saturated concentration of 4.8×10^{-3} wt% of **1** in water into consideration, the contribution of PAG molecules dissolved in water is negligible. Thus, the direct photolysis of solid particles of **1** occurs to generate HPF_6, leading to the acid-catalysed insolubilisation of PVA. It should be mentioned here that the films were only slightly turbid, when compared with the milky-white aqueous dispersion, because light scattering is effectively reduced by the better matching of the refractive index of the PVA matrix with dispersed particles when compared with water.

The type-A photopolymer was not sensitive to 365 nm light at all so that **1** was co-milled with an equimolar amount of the sensitiser (**3a**) to prepare an aqueous dispersion, which was combined with PVA and **9** to provide a type-B photopolymer. It was found that irradiation with 365 nm light makes a film of the photopolymer insoluble in water though large exposure doses of more than 6000 mJ cm^{-2} are needed, disclosing that the sensitisation through solid-state electron transfer is feasible (open circles in Fig. 9). In order to attempt improving photosensitivity, the sulfonium salt (**1**) was replaced by the iodonium (**2a**) on the basis of the results described above, considering the thermodynamic requirements for photo-induced electron transfer.[31] Consequently, an equimolar crystalline mixture of **2a** and **3a** was subjected to wet milling to formulate a type-C photopolymer. Thorough insolubilisation of a film of the photopolymer was attained at exposure doses of *ca.* 320 mJ cm^{-2}, displaying notable improvement of photosensitivity. When the molar fraction of **3a** was doubled, exposure doses were reduced down to *ca.* 120 mJ cm^{-2} (Fig. S5).[23] A SEM picture and a surface profile of a negative-type relief pattern of the type-C photopolymer showed that the relief surface is slightly rough, reflecting probably grain sizes of unreacted particles (Fig. 10). Pattern edges are more or less unsharpened probably because of an elevated post-exposure baking temperature higher than the glass transition temperature (T_g) of PVA so further optimisation is necessary.

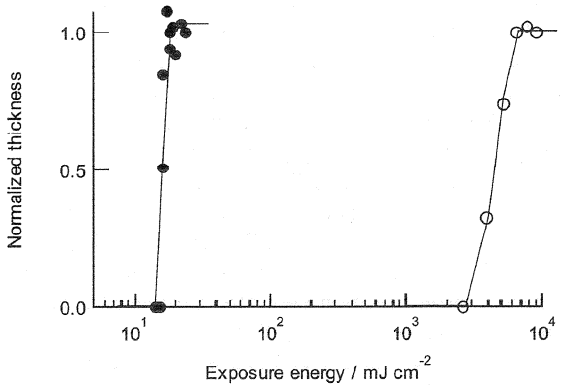

Fig. 9 Photosensitivity curves of photopolymers dispersing **1** under irradiation with 313 nm light for direct photolysis (●) and with 365 nm light for the photolysis sensitised by co-milled **3a** (○).

This journal is © The Royal Society of Chemistry 2007

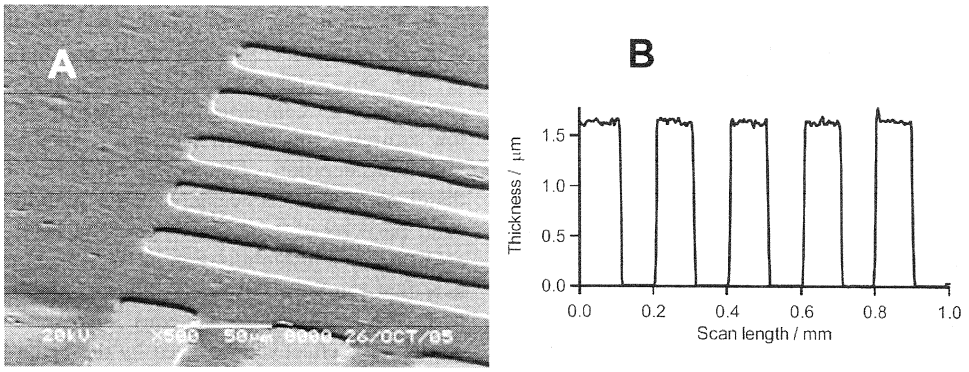

Fig. 10 (A) SEM image and (B) profile shape of a relief pattern of a PVA film containing a co-milled mixture of the PAG (**2a**) and a sensitiser (**3a**) and the epoxy crosslinker (**4**). The film was exposed to >350 nm light through a photomask, followed by heating at 120 °C for 2 min and by washing with water to remove unexposed areas.

PAG-dispersed water-borne photopolymers are now available even for the sensitised photoacid generation. The involvement of crystal-to-crystal sensitisation of **2a** as an acceptor by **3a** as a donor was furthermore confirmed by the following facts. Aqueous dispersions of **2a** and **3a** were prepared separately and mixed physically to formulate a photopolymer in such a way that concentrations of every component are the same as those of the type-C photopolymer comprising the co-milled crystalline mixture. The results are summarised in Table S3.[23] Insolubilisation was not observed at all even upon prolonged irradiation of a film of the photopolymer, revealing that a very small fraction of dissolved **2a** plays no role in displaying photosensitivity and consequently that particles of **2a** and **3a** should come in direct contact, leading to photoacid generation in line with the fluorescence quenching experiments. In this context, the separately prepared dispersions of **2a** and **3a** were combined and milled. Whereas no photosensitivity was observed for a physical mixture of both in a 1 : 1 molar ratio even after the milling, the milling of a 2 : 1 (mol : mol) mixture displayed photosensitivity though reduced by half when compared with the corresponding a 2 : 1 co-milled mixture. These results indicate that solid particles of both components are joined during the milling though the mixing efficiency is inferior when compared with the co-milled technique. This is probably because of a protective effect of PVA chains covering particle surfaces.

Photosensitivity determination was performed under irradiation with >350 nm light using the other sensitisers[32] (**3c**, **3d**, **4**, **5** and **6**), which were milled with equimolar amounts of **2a** to formulate type-C photopolymers (Table S4).[23] As summarised in Fig. 11 and Table 2, the results tell us the following. First, the nature of the sensitiser molecules influences photosensitisation efficiency considerably. **3a** and **4** work as good photosensitisers, while **3d** and **5** led to only partial insolubilisation even after prolonged irradiation. Second, sensitisation efficiency depends not only on donor and acceptor ratios, but also on particle sizes (combinations of runs 6 and 7 and of runs 8 and 9 in Table 2), suggesting that further reduction of particle sizes improves photosensitivity characteristics. In this respect, the advancement of milling technologies for nano-downsizing of organic pigment particles

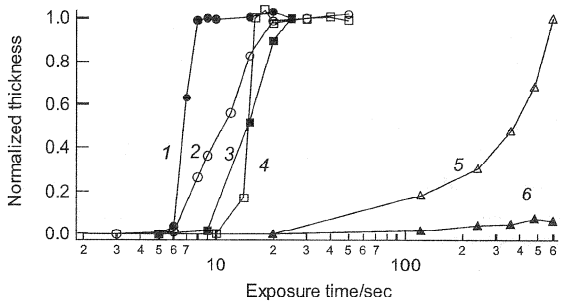

Fig. 11 Photosensitivity curves of type-C photopolymers containing dispersed **2a** co-milled with equimolar amounts of **3a** (curve-*1*, ●), **3c** (curve-*4*, □), **3d** (curve-*6*, ▲), **4** (curve-*2*, ○), **5** (curve-*5*, △) and **6** (curve-*3*, ■), respectively.

to manufacture pigment-dispersed colour filters[33] and ink-jet inks[34] may be closely related to the present subject.

Conclusions

The solid-state photolysis of scarcely water-soluble PAGs dispersed in water is applicable to the formulation of water-borne photopolymers comprised of PVA as a base

Table 2 Effects of molar ratios and particle sizes on relative photosensitivity of PAG-dispersed photopolymers upon exposure to >350 nm light

Run	Sensitiser	**2a** : Sens. (mol : mol)	Particle size/nm	PDI[a]	Relative Photosens.
1	**3a**	0.5 : 1	354	0.174	0.36
2	**3a**	1 : 1	342	0.246	1.0
3	**3a**	2 : 1	347	0.191	2.8
4	**3b**	0.5 : 1	338	0.214	0.08
5	**3b**	1 : 1	312	0.248	0.4
6	**5**	1 : 1	324	0.161	0.67
7	**5**	1 : 1	523	0.421	0.19
8	**7**	1 : 1	530	0.328	0.40
9	7	1 : 1	647	0.437	p. i.[c]

[a] Polydispersity index. [b] The photosentivity of a photopolymer doped with a 1 : 1 (mol : mol) mixture of **3a** and **2a** (run 2) is used as a standard. [c] Partial insolubilisation upon prolonged irradiation, followed by the baking.

polymer and an acid-sensitive crosslinker, providing polymerisation-type cationic photopolymers castable and developable solely with neutral water. The uniqueness of this type of PAG-dispersed photopolymer stems from the solid-state electron transfer from a sensitiser to a PAG to expand spectral sensitivity, and the results are summarised as follows.

(1) Scarcely water-soluble onium-type PAGs, water-insoluble sensitisers and mixtures of both were milled in an aqueous solution of PVA conveniently by a tabletop mill to give aqueous dispersions of particle sizes ranging from 200 nm to 500 nm under optimised conditions. Whereas the dispersions are milky-white, turbidity of cast films is reduced by better matching of the refractive index of PVA with those of organic particles when compared with water.

(2) Commercially available sensitisers exhibit characteristic photochemical events when dispersed in water. 9,10-Dialkoxyanthracene undergoes solid-state photoconversion into anthraquinone even under anaerobic conditions, whereas a thioxanthone dispersed in water displays size reduction of particles without marked photochemical reaction.

(3) The crystal-to-crystal electron transfer from sensitiser to co-milled PAG occurs to liberate strongly acidic species in aqueous dispersions when the following prerequisites are fulfilled. First, both the sensitiser and PAG crystals should be in direct contact with each other to transfer an electron from the former to the latter at the solid–solid interface through the migration of singlet or triplet excitons in sensitiser crystals. Second, the solid-state electron transfer occurs even though diameters of particles of the mixtures are in the sub-micron range, when an averaged radius of sub-grains consisting of aggregated or agglomerated particles are shorter than the exciton diffusion length.

(4) A PVA film dispersing particles of the sulfonium salt (**1**) exhibits fairly high photosensitivity of 17 mJ cm^{-2} in the presence of a water-soluble diepoxy crosslinker as a result of the direct solid-state photolysis upon exposure to 313 nm light. Whereas the sensitised photolysis of **1** results in low photosensitivity, the solid-state sensitisation of the iodonium salt (**2a**) by 9,9′-dialkoxyanthracene provides water-borne photopolymers with moderate photosensitivity of *ca.* 120 mJ cm^{-2} to 365 nm light. Photosensitivity of this kind of PAG-dispersed photopolymer is in line with solid-state fluorescence quenching efficiencies, revealing that exciton diffusion length in sensitiser crystals is one of the critical factors affecting photosensitivity performances.

Whereas the present PAG-dispersed photopolymers are applicable to micron-scale photolithography, the size reduction of PAG particles is required by all means from a practical viewpoint to improve photopolymer characteristics including photosensitivity, resolution power and optical transparency.

Acknowledgements

The author thanks the Hayashibara Biochemical Laboratories, Inc. (HBL) for the financial support and is much obliged to Mr. F. Matsui of HBL for his encouragement throughout this work.

References

1 K. Ichimura, *Heterogen. Chem. Rev.*, 1996, **3**, 419 and references therein.
2 S. Yamada, T. Mrozek, T. Rager, J. Owens, J. Rangel and C. G. Willson, *Macromolecules*, 2004, **37**, 377 and references therein.
3 (*a*) K. Ichimura, *J. Polym. Sci., Part A: Polym. Chem.*, 1982, **20**, 1411; (*b*) K. Ichimura, *Makromol. Chem.*, 1987, **188**, 2973.
4 (*a*) H. Morishita, S. Nonogaki, Y. Odaka, K. Miura and M. Nishizawa, *J. Photopolym. Sci. Technol.*, 1990, **3**, 157; (*b*) H. Morishita, M. Ito, N. Hayashi, S. Nonogaki, Y. Odaka and M. Nishizawa, *J. Photopolym. Sci. Technol.*, 1994, **7**, 59; (*c*) T. Shibuya, X. J. Rong and N. Tochizawa, *J. Photopolym. Sci. Technol.*, 1999, **12**, 377.
5 H. Ito, *Adv. Polym. Sci.*, 2005, **172**, 37.
6 J. P. Fouassier, in *Radiation Curing in Polymer Science and Technology: Fundamentals and Methods*, ed. J. P. Fouassier and J. F. Rabek, Kluwer Academic Publishers, 1994, vol. 1, pp. 49–117.
7 (*a*) Q. Lin, T. Steinhaeusler, L. Simpson, M. Wilder, D. R. Medeiros, C. G. Willson, J. Havard and J. M. J. Fréchet, *Chem. Mater.*, 1997, **9**, 1725; (*b*) J. M. Havard, S.-Y. Shim, J. M. J. Fréchet, Q. Lin, D. R. Medeiros, C. G. Willson and J. D. Byers, *Chem. Mater.*, 1999, **11**, 719; (*c*) J. M. Harvard, M. Yoshida, D. Pasini, N. Vladimirov, J. M. J. Fréchet, D. R. Mereiros, K. Patterson, S. Yamada, C. G. Willson and J. D. Byers, *J. Polym. Sci., Part A: Polym. Chem.*, 1999, **37**, 122; (*d*) J. M. Havard, N. Vladimirov, J. M. J. Fréchet, S. Yamada, C. G. Willson and J. D. Byers, *Macromolecules*, 1999, **32**, 86.
8 K. Kojima, M. Ito, H. Morishita and N. Hayashi, *Chem. Mater.*, 1998, **10**, 3429.
9 K. Naitoh, T. Yamaoka and A. Umehara, *Chem. Lett.*, 1991, **20**, 1869.
10 S. P. Pappas, M. G. Tilley and B. C. Pappas, *J. Photochem. Photobiol., A: Chem.*, 2003, **159**, 161.
11 D. Horn and J. Rieger, *Angew. Chem., Int. Ed.*, 2001, **40**, 4330.
12 K. Bitterling, M. Van der Auweraer and F. Willig, *Mater. Sci.*, 1984, **10**, 27.
13 (*a*) M. Soma, *J. Am. Chem. Soc.*, 1970, **92**, 3289; (*b*) A. Yamagishi and M. Soma, *Bull. Chem. Soc. Jpn.*, 1970, **43**, 3741.
14 E. J. Bowen, *Nature*, 1938, **3607**, 1081.
15 (*a*) O. Shimpson, *Proc. R. Soc. London, Ser. A*, 1956, **238**, 402; (*b*) H. C. Wolf, *Adv. At. Mol. Phys.*, 1967, **3**, 119; (*c*) *Photophysics of Aromatic Molecules*, J. B. Birks, Wiley-Interscience, London, 1970, pp. 528–567.
16 (*a*) C. W. Tang, *Appl. Phys. Lett.*, 1986, **48**, 183; (*b*) K. Petritsch, R. H. Friend, A. Lux, G. Rosenberg, S. C. Morrati and A. B. Holmes, *Synth. Met.*, 1999, **102**, 1776.
17 (*a*) I. Sokolik, R. Priestley, A. D. Walser, R. Dorsinville and C. W. Tang, *Appl. Phys. Lett.*, 1996, **69**, 4168; (*b*) J. Lakinowski, V. Fattori and P. Di Marco, *Chem. Phys.*, 2001, **266**, 85.
18 As preliminary reports (*a*) K. Ichimura and K. Aoki, *J. Photopolym. Sci. Technol.*, 2006, **19**, 349; (*b*) K. Ichimura and K. Aoki, *Macromol. Rapid Commun.*, in press.
19 (*a*) H. Kasai, H. S. Nalwa, H. Oikawa, S. Okada, H. Matsuda, N. Minami, A. Kakuta, K. Ono, Akio Mukoh and H. Nakanishi, *Jpn. J. Appl. Phys.*, 1992, **31**, L1132; (*b*) H. S. Nalwa, H. Kasai, S. Okada, H. Oikawa, H. Matsuda, A. Kakuta, A. Mukoh and H. Nakanishi, *Adv. Mater.*, 1993, **5**, 758.
20 (*a*) P. Kang, C. Chen, L. Hao, C. Zhu, Y. Hu and Z. Chen, *Mater. Res. Bull.*, 2004, **39**, 545; (*b*) R. O. Al-Kaysi, A. M. Müller, T.-S. Ahn, S. Lee and C. J. Bardeen, *Langmuir*, 2005, **21**, 7990.
21 K. Baba, H. Kasai, S. Okada, H. Oikawa and H. Nakanishi, *Jpn. J. Appl. Phys., Part 2*, 2000, **39**, L1256.
22 T. Seko, K. Ogura, Y. Kawakami, H. Sugino, H. Toyotama and J. Tanaka, *Chem. Phys. Lett.*, 1998, **291**, 438.
23 See electronic supplementary information†.
24 J. V. Crivello and M.-S. Jang, *J. Photochem. Photobiol., A: Chem.*, 2003, **159**, 173.
25 H. J. Timpe, K. P. Kronfeld, U. Lannel, J. P. Fouassier and D. J. Lougnot, *J. Photochem. Photobiol. A: Chem.*, 1990, **52**, 111.
26 (*a*) R. P. Swatloski, J. D. Holbrey and R. D. Rogers, *Green Chem.*, 2003, **5**, 361; (*b*) A. V. Plakhotnyk, L. Ernst and R. Schmutzler, *J. Fluorine Chem.*, 2005, **126**, 27.
27 M. Tomura, Y. Takahashi, A. Matsui and Y. Tohji, *J. Phys. Soc. Jpn.*, 1968, **25**, 647.

This journal is © The Royal Society of Chemistry 2007

28 C. L. Renschler and L. R. Faulkner, *J. Am. Chem. Soc.*, 1982, **104**, 3315.
29 G. Manivannan and J. P. Fouassier, *J. Polym. Sci., Part A: Polym. Chem.*, 1991, **29**, 1113.
30 N. P. Hacker, D. V. Leff and J. L. Dektar, *Mol. Cryst. Liq. Cryst.*, 1990, **183**, 505.
31 M. D. Soucek and J. Chen, *Proc. RadTech NA*, 2002, 13.
32 J. P. Fouassier, *Photoinitiation, Photopolymerization, and Photocuring*, Hanser Publishers, Munich, 1995, pp. 123–138.
33 (*a*) T. Komatsu and K. Ichimura, *J. Photopolym. Sci. Technol.*, 1989, **2**, 237; (*b*) R. W. Sabnis, *Display*, 1999, **20**, 119.
34 (*a*) A. D. Bermel and D. E. Bugner, *J. Imaging Sci. Technol.*, 1999, **43**, 320; (*b*) H.-K. Lee, M. K. Joyce and P. D. Fleming, *J. Imaging Sci. Technol.*, 2005, **49**, 54.

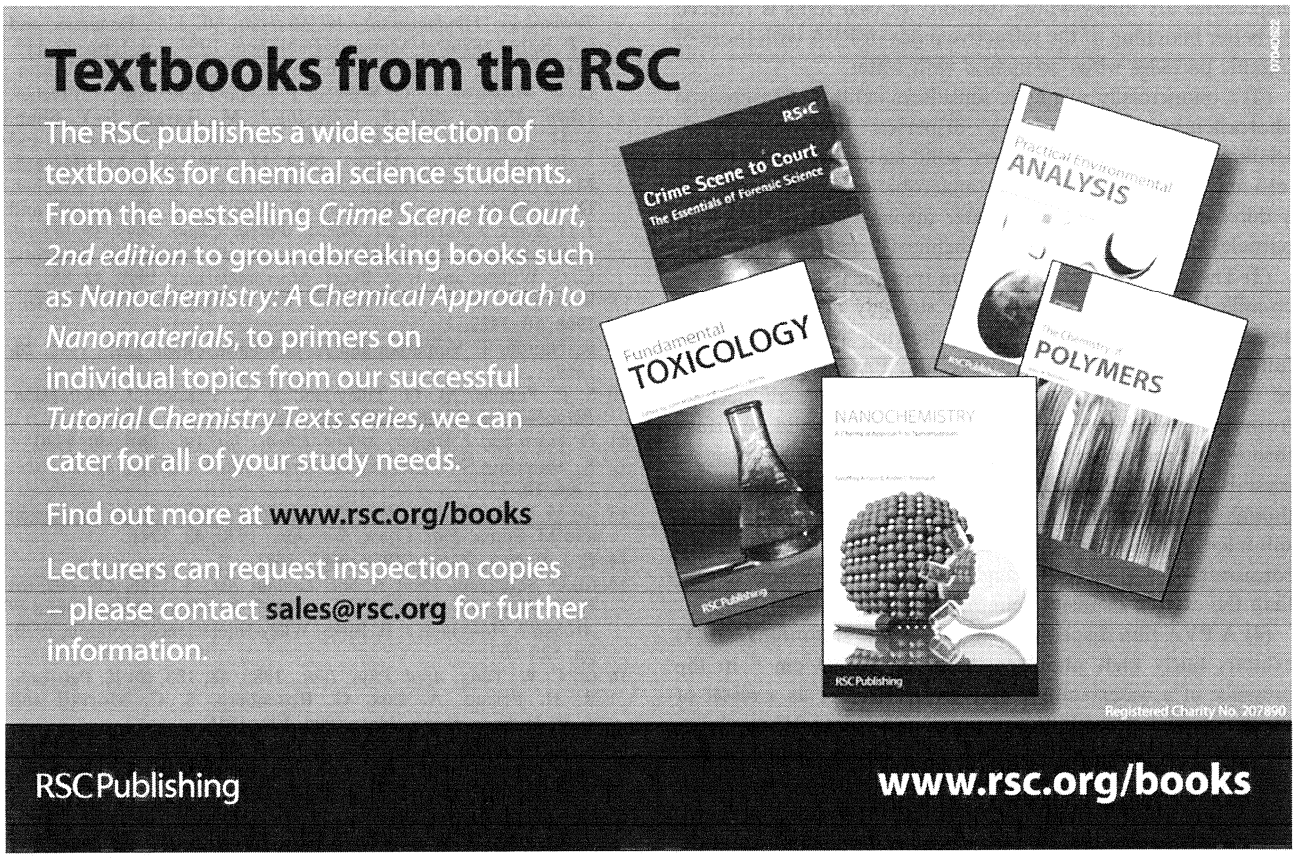

Macromolecular
Rapid Communications

Macromolecular Journals

Communication

Crystal-to-Crystal Photoinduced Electron Transfer Generating Photoacids to Formulate Water-Borne Photopolymers

Kunihiro Ichimura,* Ken'ichi Aoki

Casting a photopolymer solution to form a film, followed by imagewise photoirradiation and subsequent wet development, leads to photolithography. Whereas the wet development is achievable with aqueous alkali, the emission of an organic solvent as a volatile organic compound (VOC) is usually inevitable during the film casting because ingredients of common photopolymers are insoluble in water. We show here a prototype of water-borne photopolymers dispersed with milled nanoparticles of poorly water-soluble photoacid generators (PAGs), which undergo solid-state photolysis to liberate a photoacid to make a poly(vinyl alcohol) film insoluble in water with the aid of an acid-sensitive crosslinking reagent. The photolysis of onium-type PAGs is sensitized in the solid state simply by comilling with water-insoluble sensitizers to extend spectral sensitivity of this kind of photopolymers. Fluorescence quenching measurements revealed that the solid-state sensitization occurs through exciton migration in sensitizer particles followed by electron transfer to PAG particles.

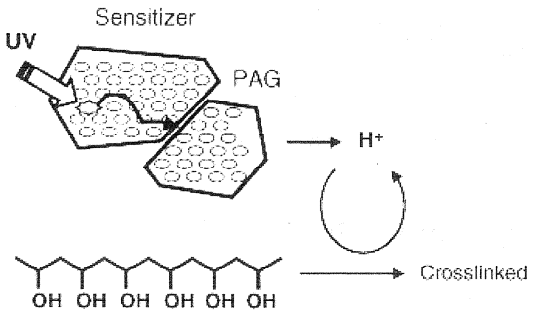

Introduction

Photolithographic processes consist of spreading a photopolymer solution to fabricate a thin film on a substrate, followed by imagewise exposure and wet development to remove unexposed or exposed areas selectively to give negative-type or positive-type relief patterns. Whereas photolithography without using any organic solvent is desirable to carry out non-volatile organic compounds (VOCs) processes, there have been only some photopolymers processed solely with neutral water.[1] Chemistries for usual photopatterning include radical or cationic photopolymerizations[2] to insolubilize an alkaline-soluble binder polymer and the acid-catalyzed deprotection of lipophilic side chains tethering to a polymer backbone with the aid of a photoacid generator (PAG) to make the polymer alkaline-soluble.[3] A radical photoinitiator or PAG liberating both cationic as well as radical species is commonly dissolved in fluid or solid solutions for these purposes. Though the wet development is achievable by using an aqueous alkali for both types of photopolymers, the emission of organic solvents is inevitable during the film casting, because photopolymers composed of a binder

K. Ichimura, K. Aoki
Faculty of Science, Toho University, 2-2-1 Miyama, Funabashi, Chiba 274-8510, Japan
Research Center for Materials with Integrated Properties, Toho University, 2-2-1 Miyama, Funabashi, Chiba 274-8510, Japan
E-mail: k-ichimura@sci.toho-u.ac.jp

Macromol. Rapid Commun. **2007**, *28*, 340–345
© 2007 WILEY-VCH Verlag GmbH & Co. KGaA, Weinheim
InterScience

DOI: 10.1002/marc.200600667

polymer, a photointiator or PAG are hardly or not soluble in water. In order to meet the requirements for non-VOC photolithographic processes, the problem stemming from the scarce water-solubility, not only of conventional PAG, but also of a sensitizer, has to be overcome to formulate water-borne photopolymers processed with neutral water for both film casting and development. In this context, aqueous dispersions of organic solid particles in the size range of nanometer to sub-micrometer[4] are very fascinating because of pseudo-solution behavior exhibiting high transparency as a result of notable suppression of light scattering. This situation motivated us to examine the solid-state direct and sensitized photolysis of onium-type PAG nano-particles dispersed in water-soluble polymer matrices to generate acidic species to devise water-borne photopolymers. We report here the photolysis of PAG in dispersions to generate acidic species to formulate a prototype of water-borne photopolymers based on the acidolytic crosslinking of poly(vinyl alcohol) (PVA) to demonstrate photolithography processed with neutral water.[5] The major concern of this paper is to deal with the particle-to-particle photoinduced electron transfer from a sensitizer to PAG leading to photoacid generation to open a general method to obtain PAG-dispersed photopolymers.

Experimental Part

Materials

Photoacid generators **(1** and **4a)** were gifted by SAN-APRO and Midori Kagaku Co., respectively, whereas **4b** was purchased from Tokyo Kasei. Sensitizers including **3b** (zone-refined), **3c**, **6**, and **8** were purchased from Aldrich, and **3a**, **3d**, **5**, and **7** were donated by Kawasaki Kasei Chemicals, Nippon Kayaku, and Midori Kagaku, respectively, and used as received.

Milling Experiments

Wet milling of a mixture of **3a** and **4a** as a typical procedure: An aqueous 5 wt.-% solution of PVA ($\overline{DP} = 500$) (9.59 g) was placed in a grinding bowl (volume; 45 mL) made of zirconia containing zirconia beads of a 3 mm diameter (10 mL), followed by adding crystals of 110.8 mg of **3a** and 302.2 mg of **4a** in a 1:1 molar ratio to be subjected to grinding at 400 rpm for 1 h by using a planetary mill (Fritsch; Pulverisette 7). Subsequently, the milling medium was replaced by zirconia beads of a 0.3 mm diameter to grind at 650 rpm for 1 h, followed by removal of the beads by filtration to give dispersed particles.

Photosensitivity Determination as a Typical Procedure

A milky-white dispersion (1.00 g) thus prepared was mixed thoroughly with 2.00 g of a 10 wt% aqueous solution of PVA ($\overline{DP} = 1700$), 32.0 mg of the diepoxy (**2**) and 0.5 g of deionized water to formulate a photosensitive composition and spin-cast on a glass plate at 1000 rpm to form an air-dried thin film. The film was exposed to 365 nm light (filters; UV-35 and UV-D35) from a Hg-Xe lamp (SAN-EI Electric Co.; UVF-203S), baked at 110 °C for 2 min and developed with neutral water to record the remaining film thickness on a profilometer (Tencor, Alpha-Step IQ) to obtain a photosensitivity curve.

Results and Discussion

To approach non-VOC photolithographic processes based on our concept, there are three steps to be exploited. The first is to achieve the nano-downsizing of PAG to reduce light scattering of their dispersions for improving optical quality of photosensitive films. The second is to corroborate the photoacid generation from PAG nano-particles thus prepared. The third is to determine whether particles of crystalline mixtures of PAG and a sensitizer undergo solid-state sensitization in polymer matrices to liberate a photoacid, since the absorption wavelengths of conventional onium-type PAG are too short to be excited directly by conventional light sources. Accordingly, we tackled to carry out wet ball-milling preliminarily by using a table-top plenary mill to grind PAG crystals with or without the sensitizer in an aqueous solution of PVA. PVA was used both as a dispersion stabilizer and a binder polymer to be crosslinked acid-catalytically. Since averaged particle sizes were influenced not only by grinding speed and period, but also by the nature of the components, appropriate milling conditions were optimized for each sample to obtain milky-white dispersions containing particles of sizes in the range from ca. 200 to 500 nm.

In order to verify the photoacid generation as a result of the solid-state photolysis of PAG particles, an aqueous dispersion of the sulfonium hexafluorophosphate (Scheme 1; **1**) was mixed with an aqueous solution of PVA containing a water-soluble epoxy compound (**2**) as an acid-sensitive crosslinker to formulate a solution of a **1**-dispersed photopolymer (type-A photopolymer), which contained **1**, PVA, and **2** in concentrations of 0.60, 6.0, and 1.00 in wt.- %, respectively. A spin-cast thin film was exposed to 313 nm light, followed by post-exposure baking to accelerate the crosslinking based on the cationic polymerization and the addition reaction of **2** to OH groups of PVA chains and development with water. Thorough insolubilization with a high contrast ratio was observed at an exposure dose of about 17 mJ cm^{-2}, exhibiting photosensitivity comparable to conventional photopolymers (Figure 1). Taking quite a low saturated concentration of 4.8×10^{-3} wt.-% of **1** in water into consideration, the contribution of PAG molecules dissolved in water is negligible, indicating that direct photolysis of solid particles of **1** occurs to generate HPF_6, leading to

© 2007 WILEY-VCH Verlag GmbH & Co. KGaA, Weinheim

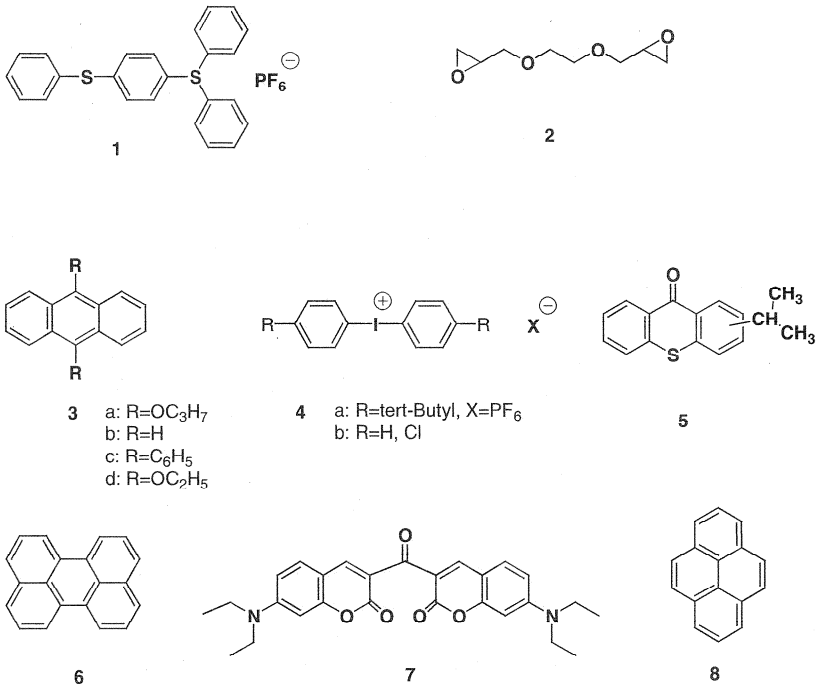

Scheme 1. Molecules employed in this study.

the acid-catalyzed insolubilization of PVA. It should be mentioned here that the films were only slightly turbid, when compared with the milky-white aqueous dispersion, because light scattering is effectively reduced because of the better matching of refractive index of PVA matrix with dispersed particles when compared with water.

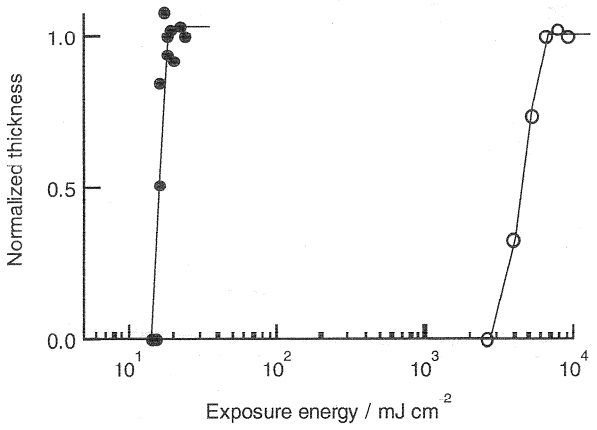

Figure 1. Photosensitivity curves of photopolymers dispersing the sulfonium salt (**1**) under irradiation with 313 nm light for direct photolysis (closed circles) and with 365 nm light for the photolysis sensitized by co-milled **3a** (open circles).

The type-A photopolymer was not sensitive to 365 nm light at all so that **1** was co-milled with an equimolar amount of the sensitizer (**3a**)[6] to prepare an aqueous dispersion which was combined with PVA and **2** to provide a type-B photopolymer. It was found that irradiation with 365 nm light makes a film of the photopolymer insoluble in water though large exposure doses of more than 6 000 mJ cm^{-2} are needed, disclosing that the sensitization through solid-state electron transfer is feasible (Figure 1). In order to attempt improving photosensitivity, the sulfonium salt (**1**) was subsequently replaced by iodonium hexafluorophosphate (**4a**), considering the thermodynamic requirements for photoinduced electron transfer.[7] Consequently, an equimolar crystalline mixture of **3a** and **4a** was subjected to wet milling to formulate a type-C photopolymer. Thorough insolubilization of a film of the photopolymer was attained at exposure doses of ca. 200 mJ cm^{-2}, displaying notable improvement of photosensitivity. When a molar fraction of **4a** was doubled, exposure doses were reduced down to ca. 70 mJ cm^{-2}. An SEM picture and a surface profile of a negative-type relief pattern of the type-C photopolymer showed that the relief surface is slightly rough, reflecting probably grain sizes of unreacted particles (Figure 2).

PAG-dispersed water-borne photopolymers are now available even for sensitized photoacid generation. The involvement of crystal-to-crystal sensitization of **4a** as an acceptor by **3a** as a donor was confirmed by the following facts. First, sensitizer crystals (**3a**) are essentially insoluble in water, whereas **4a** exhibited scarce water-solubility to give a saturated concentration of 2.5×10^{-2} wt. %, which is far low when compared with that of **4a** loaded in dispersions. Second, aqueous dispersions of **3a** and **4a** were prepared separately and mixed physically to formulate a photopolymer in such a way that concentrations of all the components are the same as those of the type-C photopolymer comprising the co-milled crystalline mixture. Insolubilization was not observed at all even upon prolonged irradiation of a film of the photopolymer, revealing that a very small fraction of dissolved **4a** plays no role in displaying photosensitivity and consequently that particles of **3a** and **4a** should come in direct contact, leading to photoacid generation. In this context, the separately prepared dispersions of **3a** and **4a** were combined and

Macromol. Rapid Commun. **2007**, *28*, 340–345
© 2007 WILEY-VCH Verlag GmbH & Co. KGaA, Weinheim
DOI: 10.1002/marc.200600667

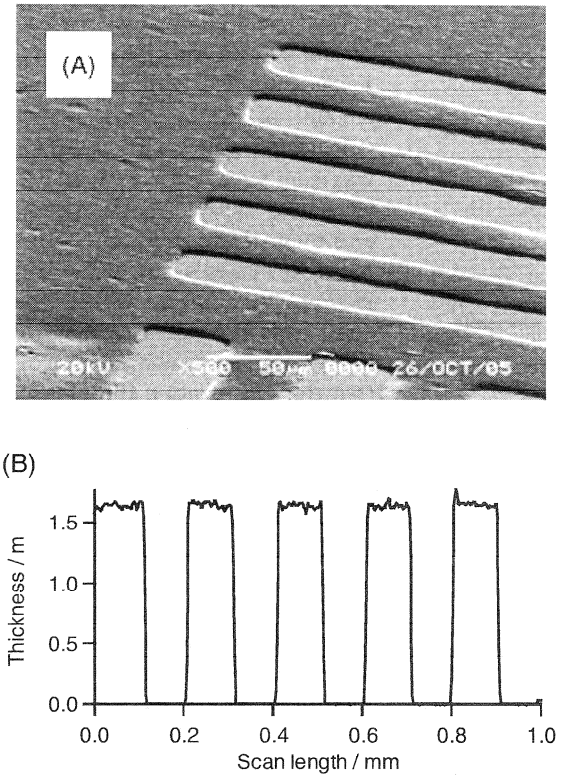

Figure 2. (A) SEM image and (B) profile shape of the relief pattern of a PVA film containing a co-milled 1:1 (mol · mol^{-1}) mixture of the PAG (**4a**) and a sensitizer (**3a**) and the epoxy crosslinker (**2**). The film was exposed to >350 nm light through a photomask, followed by heating at 120 °C for 2 min and by washing with water to remove unexposed areas.

milled. Whereas no photosensitivity was observed for a physical mixture of **3a** and **4a** in 1:1 molar ratio even after the milling, the milling of a 2:1 (mol/mol) mixture displayed photosensitivity though reduced by half when compared with the corresponding co-milled 2:1 mixture. These results indicate that solid particles of both the components are joined during the milling though the mixing efficiency is inferior when compared with the co-milled technique. This is probably because of a protective effect of PVA chains covering particle surfaces.

Photosensitivity determination was performed under irradiation with >350 nm light using other sensitizers[7] (**3b**, **3c**, **5**, **6**, and **7**), which were milled with equimolar amounts of **4a** to formulate type-C photopolymers. As summarized in Figure 3 and Table 1, we infer the following: first, the nature of sensitizer molecules influences photosensitization efficiency considerably. **3a** and **5** display higher photosensitivity, while **3c** and **6** lead only to partial insolubilization even after prolonged irradiation. Second, sensitization efficiency depends not only on a donor and acceptor ratio, but also on particle sizes (combinations of runs 6 and 7 and of runs 8 and 9 in Table 1), suggesting that further reduction of particle sizes improves photosensitivity characteristics.

In order to shed more light on the solid-state electron transfer, fluorescence quenching measurements were performed for aqueous dispersions of the anthracenes (**3**) in the presence of iodonium salts (**4**). It was found that fluorescence of a highly diluted dispersion of **3a** is quenched by water-soluble diphenyliodonium chloride (**4b**) of concentrations lower than the saturated one of 2.6 wt.-%. A Stern–Volmer constant ($k_q\tau$) in water was 8.6, whereas $k_q\tau$ for the **3a**-**4a** combination in acetonitrile solutions was 119. The results reveal the following. First, fluorescence quenching of **3a** particles by soluble **4b** can occur at a solid/water interface. Note that **3a** is dispersed even in a highly dilute aqueous solution as revealed by particle size analysis and absorption spectral measurements exhibiting a marked red shift and broadening of absorption bands. Second, assuming that a quenching constant (k_q) of **4a** is not far from that of **4b** in water, a level of fluorescence quenching by a soluble fraction of scarcely water-soluble **4a** is estimated to be 0.2% and negligibly small. This leads to an explicit idea that **4a** can act as a solid-state fluorescence quencher.

Fluorescence measurements of **3a** co-milled with **4a** to evaluate solid-state quenching efficiencies were achieved by using aqueous dispersions containing 1 wt.-% of **3a** under excitation at a 45° incidence with respect to a cell

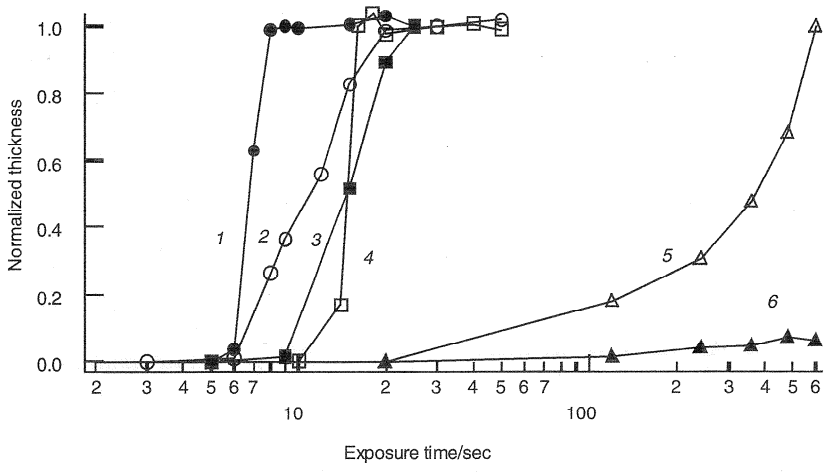

Figure 3. Photosensitivity curves of type-C photopolymers containing dispersed **4a** co-milled with equimolar amounts of **3a** (curve-1), **3b** (curve-4), **3c** (curve-6), **5** (curve-5), **6** (curve-3), and **7** (curve-2), respectively.

© 2007 WILEY-VCH Verlag GmbH & Co. KGaA, Weinheim

Table 1. Effects of molar ratios and particle sizes on relative photosensitivity of PAG-dispersed photopolymers upon exposure to >350 nm light.

Run	Sensitizer	4a:Sensitizer	Particle size	PDI[a)]	Relative photosensitivity[b)]
		mol · mol^{-1}	nm		
1	**3a**	0.5:1	354	0.174	0.36
2	**3a**	1:1	342	0.246	1.0
3	**3a**	2:1	347	0.191	2.8
4	**3b**	0.5:1	338	0.214	0.08
5	**3b**	1:1	312	0.248	0.4
6	**5**	1:1	324	0.161	0.67
7	**5**	1:1	523	0.421	0.19
8	**7**	1:1	530	0.328	0.40
9	**7**	1:1	647	0.437	p.i.[c)]

[a)]Polydispersity; [b)]Photosensitivity of a photopolymer doped with a 1:1 (mol · mol^{-1}) mixture of **3a** and **4a** (Run 2) is used as a standard; [c)]Partial insolubilization upon prolonged irradiation, followed by the baking.

surface to capture the emission from a surface layer at a 90° geometry. This is because estimating accurate absorbances at excitation wavelength of dilute dispersions were difficult due to light scattering so that the conventional 90° geometry measurement was not suitable. Since spectral shapes of fluorescence of the 1 wt.-% dispersions in shorter wavelength regions were modified due to the internal filter effect, quenching was monitored at the third peak centered at 465 nm. Furthermore, measurements were conducted quickly, since emission intensity was reduced during the excitation owing to the solid-state photosensitized conversion. Figure 4(A) shows relative fluorescence intensity (Φ/Φ_0) as a function of molar fractions of co-milled **4a**, whereas Φ and Φ_0 denote fluorescence intensity of **3a** without and with co-milled **4a**, respectively. The results disclose that the fluorescence decreases linearly with increase in molar ratio of the solid quencher. In order to reveal a general aspect of crystal-to-crystal fluorescence quenching by **4a**, aqueous dispersions of fluorescent crystals of anthracene derivatives (**3a**, **3c**, and **3d**) and pyrene (**8**) were co-milled with **4a** at various mixing ratios. The dialkoxyanthracenes (**3a** and **3d**) and **8** exhibited a linear decrease in fluorescence intensity as a function of the loading of **4a** in a way similar to **3b**. On the other hand, it should be noteworthy that the fluorescence quenching of **3c** levels off at about 30~40% so that no further quenching occurs even in the presence of excess amounts of **4a**. This makes a straightforward contrast to the fact that almost thorough quenching takes place for the others.

It is very probable that the photoinduced solid-state electron transfer takes place specifically between donor and acceptor molecules exposed to topmost surfaces of the grains. Accordingly, the diffusion of singlet exciton in sensitizer crystals[8] plays an essential role to convey excited energy to a surface donor molecule, which transfers an electron to a surface acceptor molecule through the grain boundary. First the combination of anthracene (**3b**) and **4a** is taken up for discussion, because **3b** has been one of the most extensively studied compounds for solid-state photophysics.[8] The diffusion length (DL) of singlet exciton in crystals of **3b**[9] has been reported to be in the range of 46–77 nm so that the fluorescence can be sufficiently quenched when the diameter of particles is

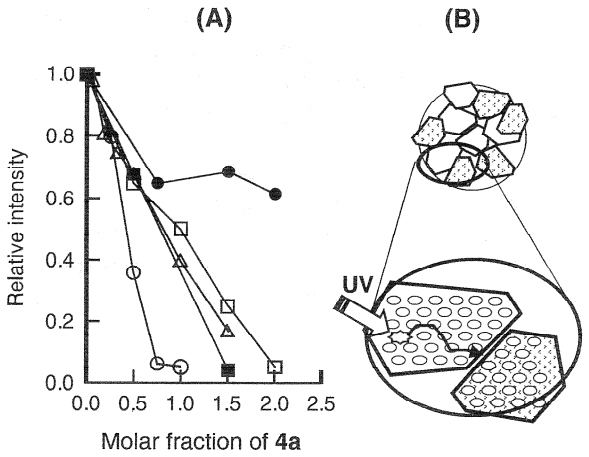

Figure 4. Solid-state fluorescence quenching in an aqueous dispersion. (A) Fluorescence intensities of particles of **3a** (open circles), **3b** (open circles), **3c** (closed circles), **3d** (open squares), and **8** (closed squares) dispersed in water as a function of weight ratios of co-milled **4a**. (B) Illustrative representation of the subparticle/exciton model for crystal-to-crystal fluorescence quenching, whereas DLS measurement detects a particle surrounded by PVA chains, which is shown as a gray circle.

Macromol. Rapid Commun. **2007**, *28*, 340–345
© 2007 WILEY-VCH Verlag GmbH & Co. KGaA, Weinheim
DOI: 10.1002/marc.200600667

shorter than DL. Thorough solid-state fluorescence quenching of the dispersed **3b** particles, with a diameter of ca. 300 nm, which is much larger than DL, can be reasonably interpreted in terms of the following. First, milled particles estimated by dynamic light scattering consist of many aggregated or agglomerated sub-particles of **3b**, diameters of which should be smaller than DL, as sketched in Figure 4(B). Second, every sub-particle of **3b** comes in intimate contact with **4a** particle(s) to result in a singlet state electron transfer. The requirement of higher weight ratios of **4a** for thorough fluorescence quenching of the other sensitizers including **3a**, **3d**, and **8** arises accordingly from DL shorter than that of **3b**, whereas no data has been available for their DL. DL of **3c** was estimated to be 5.5 nm[10] and much shorter than that of **3b** so that the solid-state electron transfer occurs only partially even under co-milling with excess amounts of **4a**. This is possibly because sub-particle sizes of **3c** fabricated are much larger than the DL value so that fluorescence quenching occurs only at a particle surface layer with a thickness corresponding to the DL value. Accordingly, the fluorescence quenching behavior is in line with quite low photosensitivity of the type-C photopolymer dispersing the **3c**-**4a** combination. Poor photosensitization efficiency of perylene (**6**) arises also from a short DL which was reported to be 0.34 nm.[9b] Concerning non-fluorescent or weakly fluorescent sensitizers for **4a**, it is known that electron transfer from thioxanthone (**5**)[11] and ketocoumarin (**7**)[12] takes place from their triplet state so that the diffusion of triplet exciton[8] in these types of sensitizer crystals plays an essential role in solid-state photosensitization.

In conclusion, solid-state electron transfer to liberate strongly acidic species in aqueous dispersions is feasible when the following prerequisites are fulfilled. First, both the sensitizer and PAG crystals should be in direct contact with each other in order to transfer an electron from the former to the latter at the solid/solid interface through the migration of a singlet or a triplet exciton in sensitizer crystals. Second, solid-state electron transfer occurs even though the diameters of particles of the mixtures are in the submicron range, when diameters of sub-grains aggregated or agglomerated in the particles dispersed in water are shorter than an exciton DL. Accordingly, quantum efficiencies for solid-state photosensitization may be improved effectively by reducing and homogenizing particle sizes of donor and acceptor mixtures in aqueous dispersions in order to hike the photosensitivity of the PAG-dispersed photopolymers processed solely by neutral water without the emission of VOC. Such a size reduction is also needed by all means from a practical viewpoint to boost photopolymer characteristics including resolution and optical transparency. To achieve this, studies on nano-downsizing of organic crystals are now in progress.

Received: September 27, 2006; Revised: November 22, 2006; Accepted: November 24, 2006; DOI: 10.1002/marc.200600667

Keywords: crosslinking; electron transfer; nanoparticles; photoacid generator; photoresists

[1] K. Ichimura, *Heterogen. Chem. Rev.* **1996**, *3*, 419.
[2] J. P. Fouassier, *"Radiation Curing in Polymer Science and Technology: Fundamentals and Methods"*, *J. P. Fouassier, J. F. Rabek, Eds.*, Kluwer Academic Publishers, Dortrecht 1994, Vol. 1, *pp.* 49–117.
[3] H. Ito, *Adv. Polym. Sci.* **2005**, *172*, 37.
[4] D. Horn, J. Rieger, *Angew. Chem. Int. Ed.* **2001**, *40*, 4330.
[5] As a preliminary report; K. Ichimura, K. Aoki, *J. Photopolym. Sci. Technol.* **2006**, *19*, 349.
[6] J. V. Crivello, M.-S. Jang, *J. Photochem. Photobiol. A: Chem.* **2003**, *159*, 173.
[7] J. P. Fouassier, *Photoinitiation, Photopolymerization, and Photocuring*, Hanser Publishers, Munich 1995, pp. 123–138.
[8] J. B. Birks, *Photophysics of Aromatic Molecules*, Wiley-Interscience, London 1970, pp. 528–567.
[9] [9a] M. Tomura, Y. Takahashi, A. Matsui, Y. Tohji, *J. Phys. Soc. Jpn.* **1968**, *25*, 647; [9b] T. Seko, K. Ogura, Y. Kawakami, H. Sugino, H. Toyotama, J. Tanaka, *Chem. Phys. Lett.* **1998**, *291*, 438.
[10] C. L. Renschler, L. R. Faulkner, *J. Am. Chem. Soc.* **1982**, *104*, 3315.
[11] H. J. Timpe, K. P. Kronfeld, U. Lannel, J. P. Fouassier, D. J. Lougnot, *J. Photochem. Photobiol. A: Chem.* **1990**, *52*, 111.
[12] G. Manivannan, J. P. Fouassier, *J. Polym. Sci., Polym. Chem.* **1991**, *29*, 1113.

© 2007 WILEY-VCH Verlag GmbH & Co. KGaA, Weinheim

Communication

Journal of Photopolymer Science and Technology
Volume 19, Number 1 (2006) 49-50 ©2006 TAPJ

Mass Transfer during Anionic UV-curing of Epoxy Resins

Ken'ichi Aoki [a,b] and Kunihiro Ichimura [a,b]

[a] *Center of Advanced photopolymers, Faculty of Science, Toho University, Chiba 274-8510, Japan*
[b] *Research Center for Materials with Integrated Properties, Toho University, Chiba 274-8510, Japan*
k-aoki@sci.toho-u.ac.jp

Keywords: mass transfer, base-proliferating reaction, oligomeric base amplifier, Oligimeric epoxy resin,

1. Introduction

Mass transfers of polymer thin films have attracted much interest and been studied mainly by using polymers containing azobenzene chromophores to form surface relief gratings.[1] Closely related phenomenon has been reported in radical polymerization of thin films of acrylates doped with a photoinitiator.[2] While several convincing models have been proposed so far, the detailed mechanism is still the subject of investigation.

Recently, we have accidentally found similar phenomenon occurring during anionic UV-curing of oligomeric epoxy resins. The process involves UV irradiation generating a catalytic amine from a photobase generator, and the subsequent heating to give rise to the base proliferation reaction (scheme 1).[3] During the post-exposure backing (PEB), a precursor called a base amplifier is autocatalytically decomposed to release a large amount of newborn amines, which promote to the crosslinking among the epoxy residues. Interestingly, during the PEB proess, marked mass migration occurred to form visible photopatterns without development with a solvent. We report here the first example of the photo-triggered mass transfer accomplished in the anionic UV-curing.

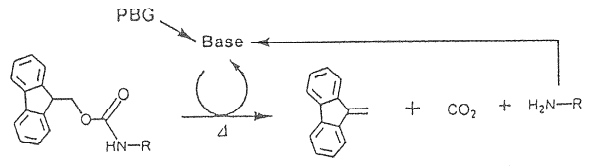

Scheme 1. Base-proliferating reaction

2. Method

Oligomeric base-amplifier of **Flu4** (Scheme 2) [4] and photobase generator (**PBG**, Scheme 2) [2a] was synthesized according to the literature methods. An oligomeric epoxy resin (**YDCN-701**, M_w = 2100, M_w/M_n = 1.58, Scheme 2) was gifted by Tohto Kasei Co.,Ltd.

Spin-cast films containing **PBG**, **Flu4**, and **YDCN-701** were exposed to 365 nm light through a photomask, followed by heating at 130 °C. Resultant patterns were observed by

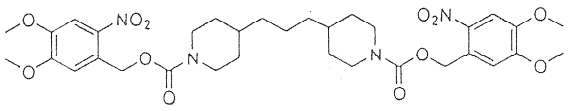

PBG

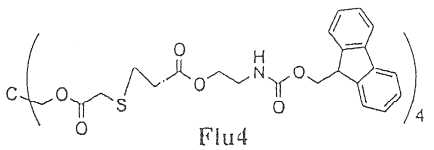

Flu4

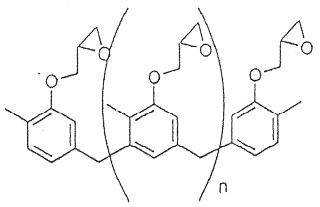

YDCN-701

Scheme 2. Chemical structures of compounds used in this study.

Received March 30, 2006
Accepted May 10, 2006

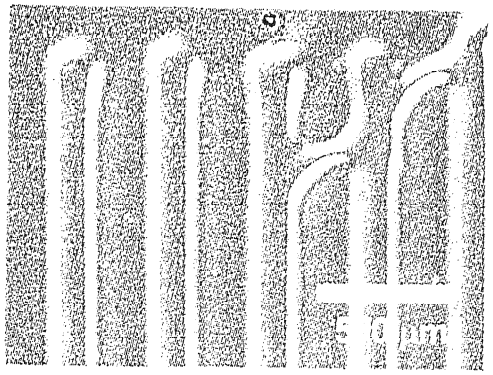

Fig. 1. Differential interference contrast microscope image of a patterned film. Exposure energy : 450 mJ cm^{-2} at 365 nm, PEB: 15 min.

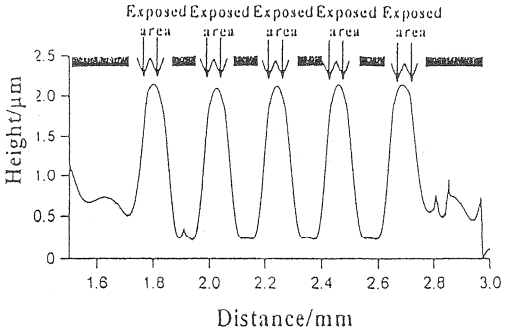

Fig. 2. Cross sectional height profile of a pattened film (L&S = 100 μm). Exposure energy : 450 mJ cm^{-2} at 365 nm, PEB: 15 min.

using a differential interference contrast microscope (Nikon, ECLIPSE/ME600), and cross sectional height profiles were measured by a surface profiler (KLA Tencor, Alpha-Step IQ).

3. Results and Discussion

Spin-cast films of *ca.* 1.2 μm in thickness were prepared from a solution containing **PBG**, **Flu4**, and the oligomeric epoxy resin. A film was exposed to 365 nm light at a 450 mJ cm^{-2} dose through a photomask, and heated at 130 °C for 15 min. Fig. 1 shows a typical example of the optical micrograph observed by a differential interference contrast microscope. It was revealed that distinct relief patterns are formed at the surface of the film. Fig. 2 displays a cross sectional height profile of the patterned film, indicating that the material at unexposed regions moves to exposed regions. Consequently, the exposed areas increase in thickness to reach to ca. 2 μm. The mechanism of the mass transfer can be explained from the viewpoint of the concentration gradients of reactive component, which promote the diffusion of the materials according to the Fick's law [2a].

The migration was found to proceed dominantly at the first stage of PEB (< 15 min.). Excess heating gave a little effect on the migration. This is because the closslinking among the epoxy residues rises a softening point of the film so that the material loses the mobility for the large-scale mass transfer. The formation of relief pattern depends markedly on the preparation conditions such as temperature and film thickness. The detailed experiments are under investigation.

Acknowledgements

This study was supported by Industrial Technology Research Grant Program (K. A; No. 04A25522d) from New Energy and Industrial Technology Development Organization (NEDO) of Japan.

References

1. (a) T. Seki, *Polymer Journal*, 36, 435 (2004). (b) T. Seki, *Handbook of Photochemistry and Photobiology*, American Scientific Publishers, 2, 435 (2003). (c) A. Natansohn and P. Rochon, *Chem. Rev.*, 102, 4139 (2002). (d) N. K. Viswanathan, D. Y. Kim, S. Bian, J. Williams, W. Liu, L. Li, L. Samuelson, J. Kumar and S. K. Tripathy, *J. Mater. Chem.*, 9, 1941 (1999). Reference to the related studies are cited therein.
2. (a) C. Croutxé-Barghorn and D. J. Lougnot, *Pure Appl. Opt.*, 5, 811 (1996). (b) C. Croutxé-Barghorn, O. Soppera and M. Chevallier, *Macromol. Mater. Eng.*, 288, 219 (2003).
3. (a) K. Arimitsu, M. Miyamoto and K. Ichimura, *Angew. Chem. Int. Ed. Engl.*, 39, 3425 (2000). (b) K. Ichimura, *Chem. Rec.*, 2, 46 (2002). (c) K. Arimitsu and K. Ichimura, *J. Mater. Chem.* 14, 336 (2004).
4. K. Aoki, K. Arimitsu and K. Ichimura, *J. Photopolym. Sci. Technol .*, 18, 133 (2005).

DOI: 10.1002/cbic.200600111

New Photoremovable Protecting Groups for Carboxylic Acids with High Photolytic Efficiencies at Near-UV Irradiation. Application to the Photocontrolled Release of L-Glutamate

Alexandre Specht,[a] Jean-Sébastien Thomann,[a] Karine Alarcon,[a] Weerawut Wittayanan,[a] David Ogden,[b, c] Toshiaki Furuta,[d] Yuji Kurakawa,[d] and Maurice Goeldner*[a]

We report here the syntheses and the photolytic properties of 3-(4,5-dimethoxy-2-nitrophenyl)-2-butyl (DMNPB) esters as new photoremovable groups for carboxylic acids, and their use for the caging of L-glutamate. A high-yielding synthesis of the DMNPB esters led to a 4:1 threo/erythro *diastereomeric mixture, which could be separated by HPLC. While these esters were stable in neutral buffer, photolysis at 364 nm induced a* $\geq$ *95% release of the carboxylic acid, with a 0.26 quantum yield for L-glutamate formation. L-Glutamate release was also possible by two-photon photolysis with an action cross section of 0.17 GM at 720 nm. Laser photolysis at 350 nm generated a transient species at around 410 nm, attributed to a quinonoid aci-nitro intermediate that decayed in the submillisecond time range ($t_{1/2}$ = 0.53 ms) for the faster γ-L-glutamyl* threo*-esters. Given the absorbance of these esters (λ_{max} = 350 nm; ε = 4500), the* threo *DMNPB esters represent new caging groups that can be efficiently photolyzed at near-UV wavelengths. An efficient and rapid photolytic release of L-glutamate has been demonstrated on hippocampal neurons in primary culture.*

Introduction

The light-induced release of a biomolecule from a caged precursor is a noninvasive method to generate a concentration jump in a time- and space-controlled manner that finds useful application mainly in cellular biology and neurobiology.[1] The criteria for the satisfactory caging of a biomolecule are well established: the appending of the photo-removable group should induce a complete loss of the biological properties, the protected compound should be soluble and stable in buffered medium, and the photolytic reaction should occur at wavelengths longer than 320 nm to avoid interference with absorbing biological molecules. Further, it should be very efficient (high product quantum yields together with high absorptivity), the photolytic side product(s) should not interfere with the ongoing photolysis and should be biologically inert, and finally, the release of the biomolecule should be fast and on the timescale of the biological event being analyzed. Among the different caging groups described in the literature, the *o*-nitrobenzyl derivatives represent by far the most developed series, even though their overall properties are often not optimal, in particular in the near-UV and visible range.

A comparative analysis of the photoremovable groups described for the caging of L-glutamate has been published recently,[2] and this survey confirmed the need for more powerful probes, despite the high number of synthesized molecules. In the *o*-nitrobenzyl series, the 1-(4,5-dimethoxy-2-nitrophenyl)-ethyl (DMNPE)[3] probes showed the expected bathochromic UV-shift, but the quantum yields were lower, as was also the case in the *p*-hydroxyphenacyl series.[4] Such a loss of photolytic quantum yields could be avoided by incorporating a trifluoromethyl group at the benzylic position,[5] but unfortunately, the corresponding carboxylic esters showed very poor hydrolytic stability. 1-Acyl-7-nitroindoline derivatives represented powerful photoremovable protecting groups for the rapid release of carboxylic acids,[6] and a MNI-caged glutamate derivative[7] was the first derivative to be described with an overall satisfactory

[a] Dr. A. Specht, J.-S. Thomann, Dr. K. Alarcon, W. Wittayanan, Prof. Dr. M. Goeldner
Laboratoire de Chimie Bioorganique–UMR 7175 LC1 CNRS
Faculté de Pharmacie, Université Louis Pasteur Strasbourg
B.P 24, 67401 Illkirch Cedex (France)
Fax: (+33) 390-244-306
E-mail: goeldner@bioorga.u-strasbg.fr

[b] Dr. D. Ogden
Laboratoire de Physiologie Cérébrale, Université René Descartes
Paris 75006 (France)

[c] Dr. D. Ogden
National Institute for Medical Research
The Ridgeway, Mill Hill NW7 1AA (UK)

[d] Prof. T. Furuta, Y. Kurakawa
Department of Biomolecular Science and Research Center for Advanced Materials with Integrated Properties, Toho University
2-2-1 Miyama, Funabashi, Chiba 274-8510 (Japan)

Supporting information for this article is available on the WWW under http://www.chembiochem.org or from the author.

 WILEY InterScience © 2006 Wiley-VCH Verlag GmbH & Co. KGaA, Weinheim

chemical and photolytic properties in the near-UV range.[8] The recent description of a 7-*N*,*N*-diethyl aminocoumarin (DECM) caged glutamate derivative extended the use of caged carboxylic acids to visible light.[9]

In this article, we describe a new photoremovable group for carboxylic acids, the 2-(4,5-dimethoxy-2-nitrophenyl)propyl (DMNPP), and the [3-(4,5-dimethoxy-2-nitrophenyl)-2-butyl] (DMNPB) esters, including the caged L-glutamate derivatives (Scheme 1). This latter group displayed outstanding photolytic efficiencies at near-UV wavelengths, and represents a useful extension of the [2-(2-nitrophenyl)propoxy] carbonyl derivatives that were described earlier for the caging of thymidine as carbonate derivatives.[10]

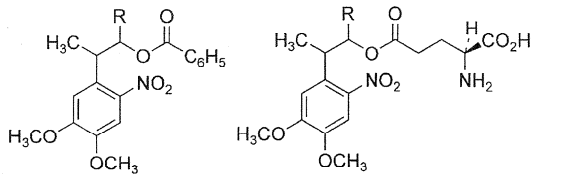

I: R = H III: R = H (DMNPP-caged L-glutamate)
II: R = CH_3 IV: R = CH_3 (DMNPB-caged L-glutamate)

Scheme 1. 2-(4,5-Dimethoxy-2-nitrophenyl)propyl (DMNPP-), [3-(4,5-dimethoxy-2-nitrophenyl)-2-butyl] (DMNPB) benzoic esters, and caged L-glutamate derivatives.

Results and Discussion

Syntheses of the DMNPP and DMNPB ester derivatives

For the synthesis of the DMNPP esters (compounds **I** and **III**) we adapted the method described in the (2-nitrophenyl)propoxy series by coupling intermediate **2** to formaldehyde under basic conditions (Scheme 2).[11] However, this method could not be extended to the coupling to aldehydes containing α-carbon hydrogens. Therefore, we developed a new approach for the synthesis of the DMNPB esters **II** or **IV**, which is also summarized in Scheme 2. The precursor alcohol **6** was synthesized in high yield (66%) in a three-step procedure starting from commercially available 3,4-dimethoxyphenyl acetone (**4**). After selective methylation of the benzylic carbon, the ketone **5** was reduced to the alcohol with $LiAlH_4$. Next, the nitro group was selectively incorporated at position 2 of the aromatic ring under mild nitrating conditions. Finally, the precursor alcohol **6** was converted to the corresponding esters by using standard procedures.

Stereochemical analysis

Reduction of the racemic methyl ketone **5** by $LiAlH_4$ generates a 4:1 mixture of the *threo*/*erythro* stereoisomers of the alcohol **6**,which can be separated by HPLC. The *threo* and *erythro* stereoisomers were identified by comparing them to samples that were individually synthesized by a Lewis acid-catalyzed opening of the *trans*- and *cis*-butene epoxide with 3,4-dimethoxyphenyl lithium, followed by nitration of the aromatic ring (Scheme 3). Unfortunately, this stereoselective epoxide-opening reaction gave very low yields despite numerous attempts, which limited the use of this two-step procedure for the synthesis of the alcohols **6**.

Stability of the DMNPB-caged Glu in buffer

The stability of the DMNPB-caged glutamate was checked by HPLC analysis of a 2×10^{-4} M solution of DMNPB-caged L-glutamate in 0.1 M phosphate buffer pH 7.2 at room temperature in the absence of light. After 24 h, less than 0.5% decomposition could be detected, indicating that neither hydrolysis of the ester, nor a β-elimination process seemed to occur in this molecule.

Photolytic studies: (Table 1)

The photolytic release of benzoic acid or L-glutamic acid from precursors **I**, **II**, or **IV** was analyzed quantitatively by HPLC after irradiation at 364 nm in neutral buffered medium. Glutamic acid formation was analyzed by means of a chromophoric derivative that was formed quantitatively after condensation with *o*-phtaldialdehyde.[12] Benzoic acid could be detected directly. In the DMNPB series, precursors **II** and **IV** released the benzoic and glutamic acids almost quantitatively (≥95%), while the DMNPP series released benzoic acid only partially (60%), despite the full conversion of the precursor **I**; this is indicative of alternative reaction pathways.

The quantum yields for glutamate release from precursors **III** and **IV** (mixture of stereoisomers) were determined by competition with the 2-(nitrophenyl)ethyl–ATP[13] reference molecule. A disappearance quantum yield of 0.36 and 0.26, respectively, could be determined from these experiments by HPLC analyses. Both DMNPP and DMNPB esters displayed high quantum yields, which conferred these molecules with high photolytic efficiencies in the near-UV range. Nevertheless, we focused the photolytic studies on the DMNPB esters because of the quantitative photorelease of glutamate.

We checked the two-photon sensitivity of the caged glutamate **IV** by irradiating the samples with a femtosecond-pulsed, mode-locked Ti–sapphire laser using a previously described method,[14] and we found an action cross section of 0.098 GM and 0.17 GM at 740 nm and 720 nm respectively. These values were similar to the one described for the MNI-caged glutamate,[15] but remain far inferior to the value described for Bhc-caged glutamate[16] (0.89 GM at 740 nm).

The fragmentation kinetics were determined after laser photolysis at 350 nm, and analysis of the decay of a transient at 410 nm. The proposed photolytic reaction mechanism[17] suggests that the rate-limiting step corresponds to the decomposition of an *o*-quinonoid *aci*-nitro intermediate (Scheme 4). Table 1 summarizes the kinetic results of the photolytic reaction performed either on the 4:1 *threo*/*erythro* mixture or on the individual stereoisomers in buffered aqueous media. The *threo* isomers displayed a monoexponential decay in the submillisecond time range ($t_{1/2}=0.53$ ms), while the *erythro* isomers displayed a biexponential kinetic carrying a slower com-

 © 2006 Wiley-VCH Verlag GmbH & Co. KGaA, Weinheim

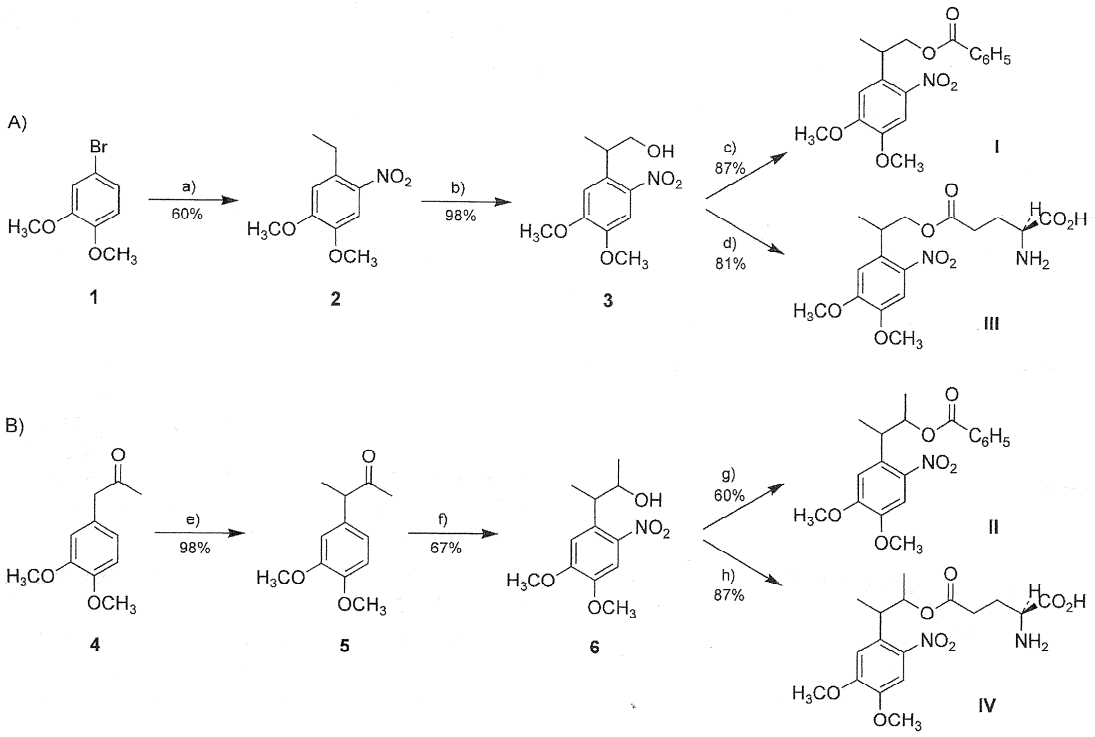

Scheme 2. Synthesis of DMNPP esters **I–IV**: i. 1) BuLi, THF, −78°C, then EtI (76%); 2) NO_2BF_4, 2-picoline, ACN (78%); ii. Triton B, $(CH_2O)_n$, DMSO, 90°C; iii. $PhCO_2H$, DCC, DMAP, $CHCl_3$; iv. 1) α-*t*-butyl *N*-BOC-L-glutamic acid, DCC, DMAP, CH_2Cl_2, (95%); 2) TFA, CH_2Cl_2, (85%); v. NaH, THF, then MeI; vi. 1) $LiAlH_4$, THF (99%), 2) NO_2BF_4, 2-picoline, ACN (68%); vii. PhCOCl, pyridine; viii. 1) α-*t*-butyl *N*-BOC-L-glutamic acid, DCC, DMAP (CH_2Cl_2), (97%); 2) TFA, CH_2Cl_2, (90%).

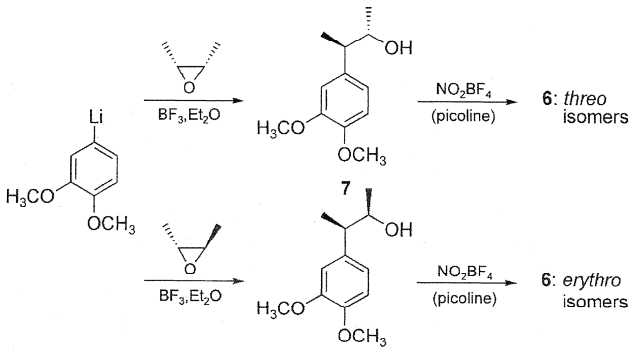

Scheme 3. Stereocontrolled syntheses of **6**.

Table 1. Photochemical parameters of DMNPP (**I**) and DMNPB (**II**, **IV**) ester derivatives.

Compound	Photoreleased acid [%]	ϕ	k [s^{-1}] (*aci*-nitro decay)
I	60	n.d.[a]	n.d.
II	95	n.d.	n.d.
III	n.d.	0.36	n.d.
IV (*threo*/*erythro* 80:20)	96	0.26	$k_1=1400$, $k_2=75$
IV (*threo* isomers)	n.d.	n.d.	$k=1300$
IV (*erythro* isomers)	n.d.	n.d.	$k_1=5000$, $k_2=80$

[a] Not determined.

ponent with a $t_{1/2}=8.6$ ms. The observed biexponential kinetics can be tentatively assigned to the *E* and *Z* isomers, but we have no satisfactory explanation for the different photolytic behavior between *erythro* and *threo* isomers. Lowering the pH from 7.2 to 6.5 did not affect these kinetics (not shown).

Biological experiments

Experiments to demonstrate the activation of glutamate receptors following photolysis of DMNPB-caged L-glutamate **IV** were made with hippocampal neurons in primary culture (Figure 1). Following whole cell voltage clamp at −70 mV photolysis of approximately 1 mM of **IV** (in 0.2% DMSO) with a flash-lamp pulse (30 mJ, 1 ms, 300–380 nm) generated a fast-rising, inward current that declined quickly initially, but then more slowly. Both AMPA and NMDA receptor subtypes were present, and experiments were done in the absence of external Mg^{2+} to permit the activation of both receptor types. The decline is likely due to the desensitization of receptors as a consequence of slow glutamate diffusion in the bath solution. The rise-time was 1.1 ms, which is similar to the flash duration, indicating rapid activation of AMPA-type receptors due to the fast release of a high glutamate concentration at the cell surface. There were no suggestions in the data that the cage itself was interfering with receptor activation. In a further series of experiments to test the physiological effects of **IV** in a brain slice preparation, a 1 M DMSO solution was prepared and applied at 1 mM to glutamatergic synaptic responses that were evoked in

 © 2006 Wiley-VCH Verlag GmbH & Co. KGaA, Weinheim

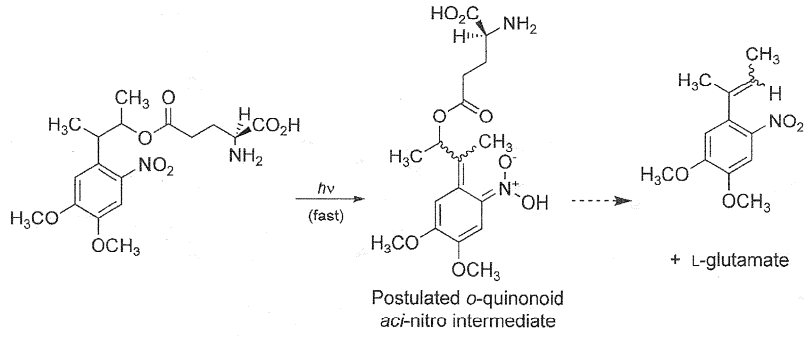

Scheme 4. Postulated photolytic mechanism for glutamate release, after ref. [17].

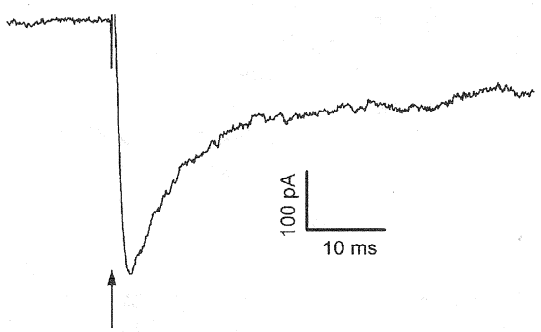

Figure 1. Response of a hippocampal neurone in primary culture to photolysis of DMNPB-caged-L-glutamate. Membrane potential −70 mV. 10–90% rise-time of glutamate-evoked current is 1.1 ms. Cage concentration 1 mm, diluted from 500 mm stock in DMSO. Light was delivered from a xenon flashlamp (1 ms pulse, 30 mJ 300-380 nm; Rapp Optoelectronic, Hamburg) through a silica condenser in the transmitted light path of a Zeiss Axioskop 1 microscope. Conversion in a single flash was estimated as being close to 100% over the cell. External solution was HEPES buffered NaCl solution pH 7.3 containing 1 μm TTx, with 2 mm Ca, 0 mm Mg ion concentrations. Internal solution contained Cs gluconate, 0.5 mm EGTA buffered with 10 mm HEPES to pH 7.3. Data was filtered at 2 kHz.

cerebellar Purkinje neurons by climbing fiber stimulation or by parallel fiber stimulation (see ref. [7] for details). The responses were suppressed, apparently due to inexcitability in the presynaptic input. Further investigation indicated that the threshold for excitation was increased, and that the Na- and K-channel components of membrane excitability were inhibited by 1 mM of **IV**, providing an explanation for the loss of presynaptic excitation observed.

Conclusion

New photoremovable groups for carboxylic acids are described, and especially the 3-(4,5-dimethoxy-2-nitrophenyl)-2-butyl (DMNPB) ester derivatives are demonstrated to be efficient caging groups for L-glutamate at near-UV irradiation. Work is in progress to use this new group for the caging of fluorophores as well as phosphoric ester-containing molecules.

Experimental Section

General: All chemicals were purchased from Sigma–Aldrich, Lancaster or Fluka in analytical grade. The NPE–ATP was purchased from Jena Bioscience. An Agilent ESI-IT-XCT+ spectrometer was used for ESI analysis. ^{1}H and ^{13}C NMR were run at 200 or 300 and 50 or 75 MHz, respectively. Coupling constants (J) are quoted in Hz and chemical shifts (δ) are given in parts per million (ppm) using the residue solvent peaks as reference relative to TMS. A Zorbax C18 column (4.6, 250 mm) was used for HPLC analyses of **I–IV** and a Acclaim C18 column (4.6× 300 mm) was used for HPLC quantum yield determination of **IV** and stereochemical analyses of **6**.

Synthesis of γ-3-(4,5-dimethoxy-2-nitrophenyl)-2-butyl-L-glutamate (DMNPB-caged Glu) IV

3-(3,4-Dimethoxyphenyl)butan-2-one (5): 3,4-Dimethoxyphenylacetone (3.78 cm^3, 21.7 mmol) was added to a stirred suspension of NaH (625 mg, 26 mmol) in dry THF (50 cm^3). After 0.5 h at room temperature, the solution was cooled to 0 °C, and iodomethane (1.49 cm^3, 23.8 mmol) was added. After 0.5 h at 0 °C, the reaction mixture was slowly allowed to reach room temperature for 1 h, and was quenched by a saturated aqueous $NaHCO_3$ solution (150 cm^3). The aqueous layer was extracted with EtOAc (3× 150 cm^3). The combined organic extracts were dried over anhydrous sodium sulfate, filtered, and concentrated in vacuo to give **5** (4.46 g, 21.4 mmol) as a yellow liquid in 98% yield. ^{1}H NMR (300 MHz, $CDCl_3$) δ = 1.38 (d, $^3J_{HH}$ = 7.1, 3H; CH_3), 2.06 (s, 3H; CH_3), 3.69 (q, $^3J_{HH}$ = 7.1, 1H; CH), 3.82 (s, 6H; 2OCH_3), 6.70 (d, $^4J_{HH}$ = 1.5, 1H; H_{ar}), 6.77–6.86 (m, 2H; H_{ar}); ^{13}C NMR (75 MHz, $CDCl_3$) δ = 17.59 (s, CH_3), 28.54 (s, CH_3CO), 53.55 (s, CH benzylic), 56.24 (s, 2OCH_3), 111.00 (s, C_{ar2}), 111.59 (s, C_{ar5}), 120.43 (s, C_{ar6}), 133.48 (s, C_{ar1}), 148.58 (s, C_{ar4}), 149.65 (s, C_{ar3}), 209.38 (s, CO).

3-(3,4-Dimethoxyphenyl)butan-2-ol (*erythro/threo* 20:80): 3-(3,4-Dimethoxyphenyl)butan-2-one **5** (1 g, 4.81 mmol) was dissolved in dry THF (15 cm^3) under argon and cooled to 0 °C. $LiAlH_4$ (200.6 mg, 5.29 mmol) was added. After 1 h at room temperature, the reaction was quenched by the addition of a saturated aqueous $NaHCO_3$ solution (150 cm^3). The aqueous layer was extracted with CH_2Cl_2 (3× 150 cm^3). The combined organic extracts were dried over anhydrous sodium sulfate, filtered and concentrated in vacuo. The residue was purified by flash chromatography (60:40 heptane/EtOAc) to give a 80:20 mixture of *threo/erythro* isomers of the product (1 g, 4.75 mmol) as a white solid in 99% yield. (for ^{1}H and ^{13}C NMR analysis of the *threo* and *erythro* isomer see the Supporting Information.

3-(4,5-Dimethoxy-2-nitrophenyl)butan-2-ol (6): NO_2BF_4 (821 mg, 6.18 mmol) was dissolved in dry acetonitrile (15 cm^3) under argon and cooled to −30 °C. 2-Picoline (0.65 cm^3, 6.72 mmol) was added slowly by using a syringe. After the mixture had been stirred for 0.5 h at −30 °C, a solution of 3-(3,4-dimethoxyphenyl)butan-2-ol (1 g, 4.76 mmol) in dry acetonitrile (5 cm^3) was added dropwise. The reaction temperature was raised slowly to reach room temperature overnight. The reaction mixture was concentrated in vacuo, and the resulting residue was dissolved in EtOAc (150 cm^3) and washed with a saturated aqueous $NaHCO_3$ solution (100 cm^3). The

 © 2006 Wiley-VCH Verlag GmbH & Co. KGaA, Weinheim

aqueous layer was extracted with EtOAc (2×150 cm^3). The combined organic extracts were dried over anhydrous sodium sulfate, filtered and concentrated in vacuo. The residue was purified by flash chromatography (90:10 to 50:50 heptane/EtOAc) to give **6** (826 mg, 3.23 mmol) as a yellow solid in 68% yield.

3-(4,5-Dimethoxy-2-nitrophenyl)butan-2-ol, *6-threo* stereoisomer: ^{1}H NMR (300 MHz, $CDCl_3$): $\delta=1.27$ (d, $^3J_{HH}=6.2$, 3H; CH_3), 1.32 (d, $^3J_{HH}=7.2$, 3H; CH_3), 3.50–3.55 (m, 1H), 3.89–3.96 (m, 1H), 3.90 (s, 3H; OCH_3), 3.93 (s, 3H; OCH_3), 6.97 (s, 1H; H_{ar6}), 7.39 (s, 1H; H_{ar3}). The HPLC retention time on a analytical C18 Acclaim (4.6×300 mm) column using a 30 min linear gradient from 0 to 100% acetonitrile in a 0.1% TFA–water solution at 1 mL min^{-1} was 20.2 min.

3-(4,5-Dimethoxy-2-nitrophenyl)butan-2-ol, *6-erythro* stereoisomer: ^{1}H NMR (200 MHz, $CDCl_3$): $\delta=1.20$ (d, $^3J_{HH}=6.1$, 3H; CH_3), 1.34 (d, $^3J_{HH}=6.8$, 3H; CH_3), 3.52–3.62 (m, 1H), 3.92–4.12 (m, 1H), 3.93 (s, 3H; OCH_3), 3.96 (s, 3H; OCH_3), 6.94 (s, 1H; H_{ar6}), 7.43 (s, 1H; H_{ar3}); ^{13}C NMR (50 MHz, $CDCl_3$): $\delta=15.44$ (s, CH_3CH), 21.90 (s, CH_3CHOH), 40.14 (s, CH benzylic), 56.67 (s, $2\times OCH_3$), 71.77 (s, CHOH), 108.21 (s, C_{ar3}), 110.70 (s, C_{ar6}), 134.57 (s,C_{ar1}), 142.63 (s,C_{ar2}), 147.45 (s,C_{ar4}), 152.87 (s,C_{ar5}). The HPLC retention time on a analytical C18 Acclaim (4.6×300 mm) column using a 30 min linear gradient from 0 to 100% acetonitrile in a 0.1% TFA–water solution at 1 mL min^{-1} was 19.8 min.

The 80:20 mixture of *threo/erythro* stereoisomers of 3-(4,5-dimethoxy-2-nitrophenyl)butan-2-ol **6** obtain by nitration of the 80:20 mixture of *threo/erythro* stereoisomers of 3-(4,5-dimethoxy-2-nitrophenyl)butan-2-ol can be separated by preparative reversed-phase HPLC on a RP18, 7 μm Symmetry shield column from Waters (19×300 mm) using a isocratic mode of 35% acetonitrile in a 0.1% TFA–water solution at 11 mL min^{-1}. The retention time of the *erythro* and *threo* stereoisomers was17 and 23 min, respectively.

α-*tert*-Butyl γ-3-(4,5-dimethoxy-2-nitrophenyl)-2-butyl *N*-BOC-L-glutamate: 3-(4,5-dimethoxy-2-nitrophenyl)butan-2-ol **6** (104.8 mg, 0.41 mmol) was dissolved in dry CH_2Cl_2 (10 cm^3) under argon. DCC (186 mg, 0.90 mmol), α-*tert*-butyl *N*-BOC-L-glutamic acid (274 mg, 0.90 mmol) and DMAP (5 mg, cat.) were added. After 5 h at room temperature, the reaction mixture was quenched with a saturated aqueous $NaHCO_3$ solution (100 cm^3). The aqueous layer was extracted with CH_2Cl_2 (3×150 cm^3). The combined organic extracts were dried over anhydrous sodium sulfate, filtered and concentrated in vacuo. The residue was purified by flash chromatography (heptane/EtOAc 80:20) to give the product (200 mg, 0.39 mmol) as a yellow solid In 96% yield.

α-*tert*-Butyl γ-3-(4,5-dimethoxy-2-nitrophenyl)-2-butyl *N*-BOC-L-glutamate *threo* stereoisomer: ^{1}H NMR (200 MHz, $CDCl_3$): $\delta=1.25$ (d, $^3J_{HH}=6.2$, 3H; CH_3), 1.31 (d, $^3J_{HH}=7.1$, 3H; CH_3), 1.43 (s, 9H; CH_3 *t*Bu), 1.44 (s, 9H; CH_3 Boc), 1.50–2.20 (m, 4H; CH_2 β and γ), 3.72–3.95 (m, 2H), 3.90 (s, 3H; OCH_3), 3.92 (s, 3H; OCH_3), 4.92 (m, 1H; NH), 5.10–5.18 (m, 1H), 6.85 (s, 1H; H_{ar6}), 7.36 (s, 1H; H_{ar3}).

α-*tert*-Butyl γ-3-(4,5-dimethoxy-2-nitrophenyl)-2-butyl *N*-BOC-L-glutamate *erythro* stereoisomer: ^{1}H NMR (200 MHz, $CDCl_3$): $\delta=1.13$ (d, $^3J_{HH}=6.1$, 3H; CH_3), 1.33 (d, $^3J_{HH}=6.8$, 3H; CH_3), 1.44 (s, 9H; CH_3 *t*Bu), 1.47 (s, 9H; CH_3 Boc), 1.40–2.45 (m, 4H; CH_2 β and γ), 3.79–4.23 (m, 2H), 3.92 (s, 3H; OCH_3), 3.95 (s, 3H; OCH_3), 5.07–5.17 (m, 2H), 6.79 (s, 1H; H_{ar6}), 7.41 (s, 1H; H_{ar3}); ^{13}C NMR (50 MHz, $CDCl_3$): $\delta=17.16$ (s, CH_3CH), 18.50 (s, CH_3CHO), 28.33 (s, CH_3 *t*Bu), 28.40 (s, CH_2 β), 28.66 (s, CH_3 Boc), 30.90 (s, CH_2 γ), 38.31 (s, CH_3CH), 53.81 (s, CH_2 α), 56.59 (s, OCH_3), 56.71 (s, OCH_3), 74.58 (s, CH_3CHO), 80.10 (s, C *t*Bu), 82.48 (s, C Boc), 108.26 (s, C_{ar3}), 110.13 (s, C_{ar6}), 132.64 (s, C_{ar1}), 142.91 (s,C_{ar2}), 147.70 (s, C_{ar4}), 153.00 (s, C_{ar5}), 156.04 (s, CO Boc), 171.66 (s, CO), 172.68 (s, CO *t*Bu).

The *erythro* stereoisomer of α-*tert*-butyl γ-3-(4,5-dimethoxy-2-nitrophenyl)-2-butyl *N*-BOC-L-glutamate was also synthesized via a Mitsunobu coupling[5] between the *threo* stereoisomer of the 3-(4,5-dimethoxy-2-nitrophenyl)butan-2-ol **6** and α-*tert*-butyl *N*-BOC-L-glutamic acid.

γ-3-(4,5-Dimethoxy-2-nitrophenyl)-2-butyl-L-glutamate (DMNPB-caged Glu) IV: α-*tert*-butyl γ-3-(4,5-dimethoxy-2-nitrophenyl)-2-butyl *N*-BOC-L-glutamate (157 mg, 0.31 mmol) was dissolved in dry CH_2Cl_2 (4 cm^3), trifluoroacetic acid (TFA) (3 cm^3) was added dropwise at room temperature. The reaction mixture was diluted with H_2O (50 cm^3) after 5 h at room temperature, and the product was extracted with EtOAc (3×100 cm^3). The combined organic extracts were dried over anhydrous sodium sulfate, filtered and concentrated in vacuo to give **IV** (103 mg, 0.27 mmol, 85%) as a yellow solid.

γ-3-(4,5-Dimethoxy-2-nitrophenyl)-2-butyl-L-glutamate (DMNPB-caged Glu) IV, *threo* stereoisomer: ^{1}H NMR (300 MHz, $CDCl_3$): $\delta=1.13$ (d, $^3J_{HH}=6.1$, 3H; CH_3), 1.29 (d, $^3J_{HH}=6.5$, 3H; CH_3), 1.95–2.45 (m, 4H; CH_2β and γ), 3.75–3.92 (m, 2H), 3.88 (s, 3H; OCH_3), 3.92 (s, 3H; OCH_3), 5.07–5.10 (m, 1H), 6.90 (s, 1H; H_{ar6}), 7.37 (s, 1H; H_{ar3}); ^{13}C NMR (75 MHz, $CDCl_3$): $\delta=17.58$ (s, CH_3CH), 17.94 (s, CH_3CHO), 26.34 (s, CH_2 β), 30.72 (s, CH_2 γ), 38.24 (s, CH_3CH), 54.32 (s, $CH_2\alpha$), 56.61 (s, $2OCH_3$), 74.71 (s, CH_3CHO), 108.14 (s, C_{ar3}), 110.57 (s, C_{ar6}), 132.18 (s, C_{ar1}), 143.20 (s, C_{ar2}), 147.62 (s, C_{ar4}), 152.97 (s, C_{ar5}), 162.52 (s, CO), 173.19 (s, CO). The HPLC retention time on an analytical SB-C18 Zorbax (4.6×250 mm) column using a 30 min linear gradient from 0 to 100% acetonitrile in 0.1% TFA–water solution at 1 mL min^{-1} was 17.0 min. The HPLC retention time on an analytical C18 Acclaim (4.6×300 mm) column using a 30 min linear gradient from 0 to 100% acetonitrile in 0.1% TFA–water solution at 1 mL min^{-1} was 18.6 min; ε_{346nm}(water) = 4100 M^{-1} cm^{-1}. ESI-MS: 385.2 $[M+H]^+$.

γ-3-(4,5-Dimethoxy-2-nitrophenyl)-2-butyl-L-glutamate (DMNPB-caged Glu) IV, *erythro* stereoisomer: ^{1}H NMR (300 MHz, $CDCl_3$): $\delta=1.04$ (d, $^3J_{HH}=6.1$, 3H; CH_3), 1.28 (d, $^3J_{HH}=6.8$, 3H; CH_3), 2.04–2.58 (m, 4H; CH_2 β and γ), 3.42–3.98 (m, 2H), 3.90 (s, 3H; OCH_3), 3.94 (s, 3H; OCH_3), 5.05–5.09 (m, 1H), 6.80 (s, 1H; H_{ar6}), 7.38 (s, 1H; H_{ar3}); ^{13}C NMR (75 MHz, $CDCl_3$): $\delta=17.12$ (s, CH_3CH), 17.87 (s, CH_3CHO), 26.19 (s, $CH_2\beta$), 31.26 (s, $CH_2\gamma$), 38.20 (s, CH_3CH), 56.62 (s, $CH_2\alpha$), 56.77 (s, $2OCH_3$), 75.33 (s, CH_3CHO), 108.33 (s, C_{ar3}), 110.40 (s, C_{ar6}), 131.80 (s, C_{ar1}), 142.89 (s, C_{ar2}), 147.71 (s, C_{ar4}), 153.09 (s, C_{ar5}), 162.50 (s, CO), 172.5 (s, CO). The HPLC retention time on an analytical SB-C18 Zorbax (4.6×250 mm) column using a 30 min linear gradient from 0 to 100% acetonitrile in 0.1% TFA–water solution at 1 mL min^{-1} was 17.0 min. The HPLC retention time on an analytical C18 Acclaim (4.6×300 mm) column using a 30 min linear gradient from 0 to 100% acetonitrile in 0.1% TFA–water solution at 1 mL min^{-1} was 18.6 min; $\varepsilon_{346\,nm}$(water) = 4100 M^{-1} cm^{-1}; ESI-MS: 385.2 $[M+H]^+$.

Quantum yield determination: The quantum yield for the photoconversion of compounds **IV**, was determined by comparison with the photolysis of 1-(2-nitrophenyl)ethyl–ATP (NPE–ATP; $\Phi=0.63$),[18] which was taken as a reference in a phosphate buffer (0.1 mM, pH 7.2) at 25 °C. These compounds were tested at identical optical densities at the reported irradiation wavelengths. Accordingly, a mixture of 0.07 mM of the DMNPB-caged Glu **IV**, or DMNPP-caged Glu **III**, and 0.2 mM of NPE–ATP reference was used. This mixture was photolyzed by continuous irradiation at 315 nm, and aliquots were subjected to reversed-phase HPLC analysis to determine the extent of the photolytic conversions. The HPLC anal-

 © 2006 Wiley-VCH Verlag GmbH & Co. KGaA, Weinheim

ysis was carried out on a Acclaim C18 column (4.6×300 nm) for **IV**, and an analytical SB-C18 Zorbax (4.6×250 mm) column for **III**; elution was performed at a flow rate of 1 mL min^{-1} with a linear gradient of acetonitrile in an aqueous solution of TFA (0.1%) from 0 to 100% (*v/v*) over 30 min. The retention times of **IV** and NPE–ATP were 18.6 and 12.9 min respectively on the Acclaim column, and the retention times of **III** and NPE–ATP were 18.1 and 14.3 min respectively on the Zorbax column. Quantum yields were calculated by considering the conversions up to 30%, to limit errors due to undesired light absorption during photolysis.

Laser flash photolysis: An excimer laser was operated at 351 nm (XeF) with a pulse energy of 100 mJ and a pulse width of about 20 ns. A pulsed Xe high-pressure arc was used as the monitoring light. A shutter disposed between the lamp and the sample cell (path-length 4 cm) was opened shortly before the laser flash to avoid photolysis of the starting compound by the Xe arc. The laser flash was perpendicular to the probing light from the pulsed Xe lamp.

Two-photon photolysis: Measurements were carried out in microcuvetts with 10×1×1 mm illuminated dimensions and 15 μL filling volume (16.10F-Q-10; Starna, Atascadero, CA). Femtosecond near IR pulses from a mode-locked, Ti–sapphire laser (Tsunami pumped by Millenium V; Spectra-Physics) were focused on the center of the sample chamber (10 mm path length) with a 25 mm focal length lens (06 LXP003/076; Melles Griot, Irvine, CA) optimized for IR lasers. The two-photon uncaging action cross section (δ_u) was estimated by referencing to fluorescein, whose fluorescence quantum yield Φ_F (0.9) and two-photon absorption cross section δ_{aF} (22 and 30 GM at 720 and 740 nm, respectively) have been characterized in the literature.[19]

The two-photon uncaging action cross section is given by Equation (1):

$$\delta_u = \frac{N_p K \Phi_F \delta_{aF} C_F}{\langle F(t) \rangle C_S} \quad (1)$$

where N_p is the number of product molecules formed per unit time (molecules/s, determined by HPLC analysis); K is the collection efficiency of our experimental setup that was used to measure the fluorescence of fluorescein emitted at a right angle to the beam and passed through a 520±10 nm bandpass filter (03FIV109, Melles Griot, Irvine, CA); C_F is the concentration of fluorescein (mol L^{-1}); $\langle F(t) \rangle$ is the time averaged fluorescence (photons/s) collected by the detector (silicon photodiode radiometer, SED033 on an IL-1700, International Light, Newburyport, MA); and *CS* is the initial concentration of the caged substrate (mol L^{-1}).

Transient spectrum detection. The detection system allowed the capture of the transient spectrum (300–600 nm) at a given time delay after excitation (time window ≥5 ns). The analyzing light was split with a prism and was focused with a lens on the entrance slit of polychromator of OMA (optical multichannel analyzer). The transient spectrum was captured by a CCD camera viewing a gateable microchannel plate image intensifier. The absorption spectrum was observed after a laser shot by using the spectral distribution of the monitoring light prior to the laser pulse as the reference light intensity at each wavelength.

Kinetics records: The detection system allowed the simultaneous capture of the kinetics at a given wavelength by using a transient digitizer. The analyzing light through the cuvette was gathered with a lens and focused on the entrance slit of a monochromator (420 nm was used to analyze the decay of the *aci*-nitro intermediate). The signal was recorded by a photomultiplier and fed into the transient digitizer. Rate constants were calculated by least-squares fitting of decay curves with single or dual exponential function, as appropriate.

For additional experimental procedures see the Supporting Information.

Acknowledgements

The authors thank Prof. Jakob Wirz and Hassen Boudebous for assistance in laser flash photolysis experiments. This work was supported by the Université Louis Pasteur and the CNRS.

Keywords: caged neurtransmitters · ester protecting groups · photolysis

[1] a) *Dynamic Studies in Biology, Phototriggers, Photoswitches and Caged Biomolecules* (Eds.: M. Goeldner, R. Givens), Wiley-VCH, Weinheim, **2005**; b) A. P. Pelliccioli, J. Wirz, *Photochem. Photobiol. Sci.* **2002**, *1*, 441–458; c) G. Marriott, J. Ottl, M. Heidecker, D. Gabriel, *Methods Enzymol.* **1998**, *291*, 95–116.

[2] "Photoremovable Protecting Groups Used for the Caging of Biomolecules. Caging of ATP and Glutamate: Comparative Analyses" M. Goeldner in *Dynamic Studies in Biology, Phototriggers, Photoswitches and Caged Biomolecules* (Eds.: M. Goeldner, R. Givens), Wiley-VCH, Weinheim, **2005**.

[3] J. W. Wootton, D. R. Trentham, *NATO ASI Ser. C* **1989**, *272*, 277–296.

[4] P. G. Conrad II, R. S. Givens, J. F. W. Weber, K. Kandler, *Org. Lett.* **2000**, *2*, 1545–1547.

[5] A. Specht, M. Goeldner, *Angew. Chem.* **2004**, *116*, 2042–2046; *Angew. Chem. Int. Ed.* **2004**, *43*, 2008–2012.

[6] G. Papageorgiou, D. C. Ogden, A. Barth, J. E. T. Corrie, *J. Am. Chem. Soc.* **1999**, *121*, 6503–6504.

[7] M. Canepari, L. Nelson, G. Papageorgiou, J. E. T. Corrie, D. Ogden, *J. Neurosci. Methods*, **2001**, *112*, 29–42.

[8] J. Morrison, P. Wan, J. E. T. Corrie, G. Papageorgiou, *Photochem. Photobiol. Sci.* **2002**, *1*, 960–969.

[9] V. R. Shembekar, Y. Chen, B. K. Carpenter, G. P. Hess, *Biochemistry* **2005**, *44*, 7107–7114.

[10] S. Bühler, I. Lagoja, H. Giegrich, K-P. Stengele, W. Pfeiderer, *Helv. Chim. Acta* **2004**, *87*, 620–659.

[11] A. Hasan, K-P. Stengele, H. Giegrich, P. Cornwell, K. R. Isham, R. A. Sachleben, W. Pfeiderer, R. S. Foote, *Tetrahedron* **1997**, *53*, 4247–4264.

[12] R. F. Chen, C. Scott, E. Trepman, *Biochim. Biophys. Acta* **1979**, *576*, 440–445.

[13] J. W. Walker, G. P. Reid, J. A. McCray, D. R. Trentham, *J. Am. Chem. Soc.* **1988**, *110*, 7170–7177.

[14] T. Furuta, S. S. Wang, J. L. Dantzker, T. M. Dore, W. J. Bybee, E. M. Callaway, W. Denk, R. Y. Tsien, *Proc. Natl. Acad. Sci. USA* **1999**, *96*, 1193–1200

[15] M. Matsuzaki, G. C. R. Ellis-Davies, T. Nemoto, Y. Miyashita, M. Iino, H. Kasai, *Nat. Neurosci.* **2001**, *4*, 1086–1092.

[16] T. Furuta, S. S.-H. Wang, J. L. Dantzer, T. M. Dore, W. J. Bybee, E. M. Callaway, W. Denk, R. Y. Tsien, *Proc. Natl. Acad. Sci. USA* **1999**, *96*, 1193–1200.

[17] S. Walbert, W. Pfleiderer, U. E. Steiner, *Helv. Chim. Acta* **2001**, *84*, 1601–1611.

[18] J. W. Walker, G. Reid, J. A. McCray, D. R. Trentham, *J. Am. Chem. Soc.* **1988**, *110*, 7170–7177.

[19] C. Xu, W. W. Web, *J. Opt. Soc. Am. B* **1996**, *13*, 481–491.

Received: March 22, 2006
Published online on September 22, 2006

 © 2006 Wiley-VCH Verlag GmbH & Co. KGaA, Weinheim

Acta Crystallographica Section E
Structure Reports Online
ISSN 1600-5368

1,7-Bis(1,3-dimethyluracil-6-yl)-1,4,7,10-tetraazacyclododecane acetonitrile disolvate at 100 K

Akira Uchida,[a]* Ayako Komori[a] and Soichiro Watanabe[a,b]

[a]Department of Biomolecular Science, Faculty of Science, Toho University, Miyama 2-2-1, Funabashi, Chiba 274-8510, Japan, and [b]Research Center for Materials with Integrated Properties, Toho University, Miyama 2-2-1, Funabashi, Chiba 274-8510, Japan

Correspondence e-mail: auchida@biomol.sci.toho-u.ac.jp

Received 26 December 2006
Accepted 5 January 2007

Key indicators

Single-crystal X-ray study
T = 90 K
Mean σ(C–C) = 0.002 Å
R factor = 0.035
wR factor = 0.094
Data-to-parameter ratio = 17.3

For details of how these key indicators were automatically derived from the article, see http://journals.iucr.org/e.

The title compound [systematic name: 1,1′,3,3′-tetramethyl-1,1′,2,2′,3,3′,4,4′-octahydro-6,6-(1,4,7,10-tetraazacyclododecane-1,7-diyl)dipyrimidine-2,2′,4,4′-tetraone acetonitrile disolvate], $C_{20}H_{32}N_8O_4\cdot 2CH_3CN$, an *N*-uracil-substituted cyclen derivative, is located on a crystallographic twofold rotation axis running through the center of the 12-membered ring and adopts a [3333] quadrangular conformation with C atoms occupying the corners.

Comment

Cyclen (1,4,7,10-tetraazacyclododecane) is one of the most important macrocycles as a metal-chelating ligand (Curtis, 2004). Numerous *N*-alkyl cyclen derivatives have been reported to improve their affinity, modify their metal-chelating properties, prepare MRI contrast reagents (Gries & Schering, 2002), and so on. However, there are few reports on *N*-aryl-substituted cyclen derivatives because an efficient general synthetic approach is lacking (Michael & Burkhart, 2001). We report here the structure of compound, (I), prepared in the course of our studies on new *N*-aryl-substituted cyclen derivatives.

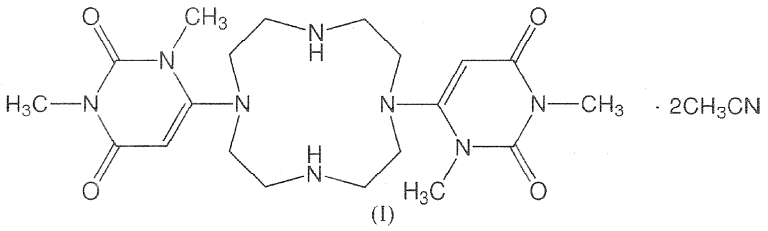

(I)

The molecule possesses twofold rotation symmetry, the axis of which passes through the center of the 12-membered cyclen ring (Fig. 1). The cyclen ring assumes a [3333] quadrangular conformation with four repeating units, each containing two succesive *gauche* and one *anti* conformations (Table 1). All four N atoms of the cyclen ring lie on one side of the mean plane through the macrocycle. Due to the steric hindrance caused by the dimethyluracil group at N1, the N1—C1 and N1—C4^{i} distances are significantly longer [1.4814 (13) and 1.4972 (13) Å, respectively; symmetry code: (i) $1-x, y, \frac{1}{2}-z$] than the N2—C2 and N2—C3 distances [1.4659 (13) and 1.4627 (13) Å, respectively], and C5 of the uracil ring lies out of the mean plane by 0.440 (1) Å.

Experimental

A solution of cyclen (3.53 mmol), 1,3-dimethyl-6-chlorouracil (7.50 mmol) and sodium carbonate (7.03 mmol) in acetonitrile

© 2007 International Union of Crystallography
All rights reserved

(25 ml) was stirred overnight under reflux. After filtration of the inorganic salt, a white solid of (I) precipitated from the filtrate (yield 61%, 2.15 mmol). Single crystals were obtained from an acetonitrile solution.

Crystal data

$C_{20}H_{32}N_8O_4{\cdot}2C_2H_3N$
M_r = 530.64
Monoclinic, $C2/c$
a = 24.2718 (18) Å
b = 7.5477 (6) Å
c = 14.3193 (11) Å
β = 92.4510 (10)°
V = 2620.8 (3) Å^3
Z = 4
D_x = 1.345 Mg m^{-3}
Mo $K\alpha$ radiation
μ = 0.10 mm^{-1}
T = 100 (1) K
Block, colorless
0.40 × 0.40 × 0.25 mm

Data collection

Bruker APEX-II CCD diffractometer
φ and ω scans
Absorption correction: multi-scan (*SADABS*; Sheldrick, 1996)
T_{min} = 0.963, T_{max} = 0.977
7243 measured reflections
3096 independent reflections
2681 reflections with $I > 2\sigma(I)$
R_{int} = 0.015
θ_{max} = 28.7°

Refinement

Refinement on F^2
$R[F^2 > 2\sigma(F^2)]$ = 0.035
$wR(F^2)$ = 0.094
S = 1.04
3096 reflections
179 parameters
H atoms treated by a mixture of independent and constrained refinement
$w = 1/[\sigma^2(F_o^2) + (0.0465P)^2 + 1.6563P]$ where $P = (F_o^2 + 2F_c^2)/3$
$(\Delta/\sigma)_{max}$ = 0.001
$\Delta\rho_{max}$ = 0.28 e Å^{-3}
$\Delta\rho_{min}$ = −0.21 e Å^{-3}

Table 1
Selected geometric parameters (Å, °).

C3—C4	1.5232 (14)	C2—C1	1.5287 (14)
C1—N1—C4^i	112.48 (8)	C3—N2—C2	113.65 (8)
N2—C3—C4—N1^i	73.27 (11)	C4^i—N1—C1—C2	−150.35 (8)
C4—C3—N2—C2	−170.94 (8)	N2—C2—C1—N1	60.59 (11)
C1—C2—N2—C3	70.45 (11)	C1—N1—C4^i—C3^i	70.80 (10)

Symmetry code: (i) $-x+1, y, -z+\frac{1}{2}$.

All H atoms were located in a difference Fourier map. Except for the imino H atom, they were repositioned in calculated positions (C—H = 0.93–0.98Å) and refined as riding, with U_{iso}(H) = 1.2U_{eq}(C). For the imino H atom, the N—H distance was restrained to 0.86 (1)Å and the isotropic displacement parameter was refined freely.

Data collection: *APEX2* (Bruker–Nonius, 2004); cell refinement: *APEX2*; data reduction: *SAINT-Plus* (Bruker–Nonius, 2004); program(s) used to solve structure: *SHELXS97* (Sheldrick, 1997); program(s) used to refine structure: *SHELXL97* (Sheldrick, 1997); molecular graphics: *PLATON* (Spek, 2003) and *ORTEPIII* (Burnett & Johnson, 1996); software used to prepare material for publication: *SHELXL97* and *PLATON*.

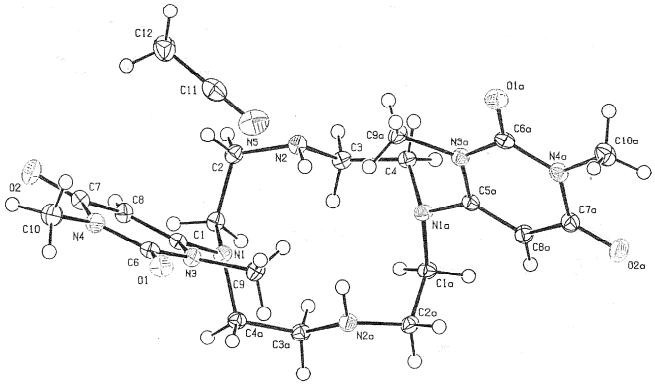

Figure 1
The molecular structure of (I), showing displacement ellipsoids drawn at the 50% probability level. H atoms are represented as spheres of arbitrary radius. The suffix a corresponds to symmetry code (i) in Table 1.

References

Bruker–Nonius (2004). *APEX2* and *SAINT-Plus*. Bruker–Nonius BV, Delft, The Netherlands.
Burnett, M. N. & Johnson, C. K. (1996). *ORTEPIII*. Report ORNL-6895. Oak Ridge National Laboratory, Tennessee, USA.
Curtis, N. F. (2004). *Comprehensive Coordination Chemistry II*, Vol. 1, edited by J. A. McCleverty & T. J. Meyer, pp. 447–474. Oxford: Elsevier.
Gries, H. & Schering, A. G. (2002). *Top. Curr. Chem.*, **221**, 1–24.
Michael, S. & Burkhart, K. (2001). *Synthesis*, pp. 1818–1825.
Sheldrick, G. M. (1996). *SADABS*. University of Göttingen, Germany.
Sheldrick, G. M. (1997). *SHELXS97* and *SHELXL97*. University of Göttingen, Germany.
Spek, A. L. (2003). *J. Appl. Cryst.* **36**, 7–13.

先端技術

ナノテク成果 世界が注目

触媒などに使われる「メソ多孔体」、金属結晶を超微細化した高強度材料……。研究者が注目する日本人研究者の論文は、ナノテクノロジー（超微細技術）に関する成果が目立った。二十一世紀に入り、様々な分野で起きた日本のナノテク研究ブームを反映した形となった。（1面参照）

化学 メソ多孔体解析

ストックホルム大学 寺崎治 教授

化学分野で最も論文が引用された寺崎治ストックホルム大学教授は、「メソ多孔体」と呼ばれる小さな穴が空いた材料の構造を電子顕微鏡で詳しく解析、材料の形状や特性を調べる。寺崎教授は電子顕微鏡で微細な構造を正確に解析する技術を持つ。

メソ多孔体は約二百ナノ（ナノは十億分の一）mの穴が多数空いたシリカゲルなどの材料。穴の中に白金などを入れ、薬物送達システム（DDS）や触媒材料などに使われ、応用範囲は広い。寺崎教授は東北大学時代に電子顕微鏡の技術を開発。穴の大きさなどを詳しく調べて新材料の開発に生かすもので、研究基盤技術となるだけに世界の注目が集まっている。

東大 藤田誠 教授

メソ多孔体の研究開発は世界でも日本人の研究者が先頭を走る。早稲田大学や豊田中央研究所などが研究に取り組み、寺崎教授の論文引用数を押し上げた。

二位となった藤田誠東大教授は、ナノメートルサイズの特殊な構造を持つ分子を合成する。複数の分子が自発的に構造を作る「自己組織化」という現象を利用し、直径一ナノのかご状の物質などを作った。この内部では普通では起きないような特殊な化学反応が起きる。医薬品や農薬、燃料や有機分子が結合した新材料を開発した。天然ガスやメタンを低圧でためる吸着材料として応用が期待されている。大阪ガスと共同で、フォークリフトやバイクの燃料用タンクなどへの実用化を進めている。

京大 北川進 教授

材料科学 金属ガラス発明

東北大金属材料研究所長 井上明久 氏

材料分野で一位となった東北大学金属材料研究所の井上明久所長（教授）は、原子が不規則に並んだアモルファス（非晶質）金属を研究する。冷却して作るこの材料は「金属ガラス」と呼ばれ、耐熱性や耐食性に優れた特性を生かして超小型モーターや医療用器具などに応用が進む。

最近は中国やインドなどのアジア諸国でも金属ガラスの研究開発が進むなど、研究者のすそ野が広がっており、引用件数を押し上げたとみられる。

九州大 堀田善治 教授

九州大学の堀田善治教授らは熱処理などで金属ソフトは「リートベルト法」と呼ばれる計算手法を応用、粉末材料の結晶構造を正確に調べられる。日本語版としてインターネットを通じて無料で配布して、燃料電池や超電導の研究者が利用している。

物材機構 主席研究員 泉富士夫 氏

物質・材料研究機構の泉富士夫主席研究員は無機材料の構造を解析するソフトウエアを開発、そのソフトを利用した論文が引用数を押し上げた。

一方、材料科学の世界一位は、カーボンナノチューブ（筒状炭素分子）の研究で知られるペイドン・ヤン米カリフォルニア大学バークレー校準教授だった。二〇〇〇年以降、世界で本格的に研究が始まったナノテクノロジーの活況を示した調査結果となった。

論文の引用数 本社調査

調査の概要　自然科学系の主要学術誌に二〇〇〇年から〇五年八月までに掲載された論文が、他の論文にどれだけ引用されたかを調べた。今回は主要化学誌に掲載された約六千の論文と、材料科学誌の約二千の論文を調査の対象とした。

引用数が多いほど世界の研究者に影響を及ぼした論文とされる。発表時期の古い論文が多いほど回数が多くなる傾向がある。また研究者人口の多い分野は論文の引用数も多くなりやすい。

化学と材料科学分野で論文の被引用件数の多い研究者

		総引用数	論文数	研究代表者	研究テーマ
化学分野	1位	1,369	10	寺崎治スウェーデンストックホルム大学教授	メソ多孔体
	2位	1,058	11	藤田誠東京大学教授	ナノ化学
	3位	743	12	北川進京都大学教授	金属と有機分子の化合物
	4位	647	11	林民生京都大学教授	ロジウム触媒
	5位	611	13	柴崎正勝東京大学教授	不斉合成触媒
	世界1位	2,299	15	ロバート・グラブス米カリフォルニア工科大教授	メタセシス触媒
材料科学分野	1位	1,175	13	井上明久東北大学金属材料研究所長	アモルファス金属
	2位	603	12	堀田善治九州大学教授	金属結晶の微小化
	3位	368	2	泉富士夫物質・材料研究機構主席研究員	粉末材料の解析ソフト
	4位	254	2	市村國宏東邦大学特任教授	光機能材料
	5位	238	4	新海征治九州大学教授	ナノ化学
	世界1位	1,217	12	ペイドン・ヤン米カリフォルニア大学準教授	ナノチューブ

科学技術

東邦大が新感光性材料

露光・加熱でパターン形成

塩基増殖反応でオリゴマー移動　溶剤現像が不要に

東邦大学複合物性研究センターの市村國宏理学部特任教授と青木健一理学部講師は、露光と加熱だけでパターン形成する感光性材料を開発した。塩基（アミン）増殖反応を利用した物質移動によるパターン形成技術で、露光後、加熱によって架橋剤のポリアミンが露光部だけで飛躍的に生成し、エポキシオリゴマーを架橋して硬化する。一方、未露光部の未反応オリゴマーは露光部に移動して架橋されるため、露光と加熱だけでパターンを形成する。今後、有機溶剤による現像（未反応材料の除去）が不要な環境低負荷型感光性材料としてプリント配線基板などへの応用を目指す。これは今年度の新エネルギー・産業技術総合開発機構（NEDO）の産業技術研究助成事業の一環として得られた成果で、三十日、千葉大学西千葉キャンパスで開かれる第二十三回フォトポリマーコンファレンスで発表する。

開発した感光性材料は光塩基（アミン）発生剤、架橋剤となる塩基増殖オリゴマー、ノボラック型エポキシオリゴマーで構成している。これを有機溶媒（ポリアミン）に溶かし、通常のスピンコートでガラス基板上に成膜、パターン露光（波長三百六十五ナノメ）する。露光と加熱によって露光部だけでオリゴマーの架橋が起こり、パターンを形成する。メカニズムは露光によって露光部だけで光塩基発生剤からアミンが生成。このアミンが起爆剤として塩基増殖オリゴマーが自らもアミンを作り出しながら、連鎖的にポリアミンに変化、エポキシオリゴマーを架橋する。さらに未露光部ではアミンがないためエポキシオリゴマーは未反応で、露光部との濃度こう配により露光部に移動して架橋反応を起こす。加熱条件は百三十度Cで二十分。

エポキシオリゴマーの分子量は二千百と通常のポリマーより一ケタ小さいことから、未露光部からの移動が起こったと推測される。移動距離は〇・三一〇・四マイクロメートル程度。現在は未露光部に未反応材料が残っているが、露光部（パターン部分）が盛り上がっているので、未露光部との高低差は大きく、そのままでもプリント配線基板などのエッチングができる可能性はある。今後、分子量、材料構成、反応条件などの最適化を行い、未露光部に材料が残らない有機溶媒による現像が不要な感光性材料の開発にも取り組む。

なるほど！化学アカデミー

3時間目　浮き上がる感光性材料

光と熱で〝物質移動〟その力をそのまま使うと…

物質は光や熱によってかたくなったり、やわらかくなったりと、その性質を変化させることができます。これは物質を構成する成分が光や熱という刺激を受け、物質の構造を変えるためです。その力をそのまま生かして、思うようなかたちにしたり、人の手を加える必要が少なくなれば、モノを作るときのエネルギーを節約したりするのに役立つはずです。東邦大学複合物性研究センターの青木健一理学部講師は、光が当たった部分が熱によって浮き上がる、これまでにない感光性材料を発見しました。薄い膜になっているその材料では、光の当たっていない部分が光に当たっている部分へ集まっていくことを突き止めました。青木さんは、携帯電話などに使われるプリント配線板を作る、環境にやさしい材料として実用化に取り組んでいます。

薬品が不要になる

これまでにも物質移動する材料は知られていますが、この感光性材料はまったく新しい種類のものでした。移動距離は0・二㍉㍍から0・四㍉㍍と大きいのも特徴です。これが実用化されると、パソコンや携帯電話などに使われる「プリント配線板」を作るとき、薬品を使わなくてもよくなるかもしれません。

パソコンや携帯電話などの電子機器のなかをのぞくと、たくさんの小さな部品が板のうえにのっています。これがプリント配線板です。この板には電気が流れる細い〝線の線〟があって、電子回路を形成しています。感光性材料は、この微細な線の線を作る時などに使います。線の薄い板（銅箔）に感光性材料の薄い膜を作り、そこに光で電子回路のパターンを描きます。これを「露光」といいます。光の当たった部分の感光性材料はかたくなり、当たらなかった部分はそのままです。

次に、光の当たらなかった感光性材料を有機溶媒という薬品で洗い落とし、かたくなった部分だけを残します。これを「現像」といい、そのパターンにそって、不必要な部分の銅箔を取り除きます（エッチング）。残った銅箔部分がプリント基板の電気回路となるのです。

新しい感光性材料は、光が当たった部分が加熱されると光が当たった部分が浮き出る不思議な材料です。これは光が当たらなかった（未露光）部分が光の当たった（露光）部分に移動するためです。未露光部から感光性材料が全部なくなってしまえば、薬品を使った現像が不要となります。薬品が不要となるわけですから、環境にやさしい材料といえます。

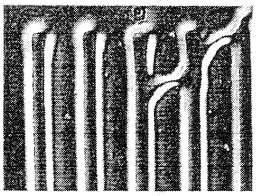
新しい感光性材料で作られたパターン

濃度の差がカギに

なぜ、このようなことが起こるのでしょうか？最初に感光性材料はアミンは飛びません。次に膜全体に熱をかけると、熱がスイッチとなって、アミンが膜に入っている物質を使ってポリアミンと呼ばれるものを作り、これが膜の成分をかたく（硬化）させます。

ここで「物質移動」という現象が起こります。物質移動は、濃度が濃い方から薄い方に移動して濃度を一定にする物質の性質が原理となっています。これを今回の感光性材料に当てはめると、露光部分では、どんどん硬化という反応が進んで材料が減っていきます。一方、未露光部分は硬化反応が起こりませんから、材料はそのままです。これを材料の濃度で考えると、未露光部分が濃く露光部分が薄いことになり、未露光部分から材料が移動して露光部分が盛り上がることになります。実験ではまだ、未露光部分の材料がすべて露光部分に移動するほどの結果は出ていません。

〔表面レリーフの形成機構〕

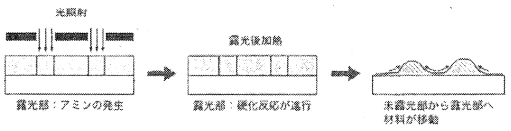

研究は終わらない

物質のなかでは、とても不思議なことが起こっています。新しい材料を作ることは化学の研究ですが、現象がどのように起こるかを突き止めることも化学の研究です。研究はこれで終わりではありません。未露光部分の材料が全部移動するなど、もっと大きく移動する感光性材料の研究に取り組むとともに、環境にやさしいといった、世の中に役立つ材料開発に成戦していきます。

担当は　青木　健一　先生

青木健一（あおき・けんいち）さんは香川県出身。研究者を目指したのは小学校の頃、「楽しかった」理科の実験がきっかけだそうです。もちろん中学、高校では化学や物理は得意で、「英語も好き」でした。大学は「ここで勉強したい」と心に決めていた千葉大学工学部画像工学科に入学、東京工業大学総合理工学研究科で博士号を取得、産業技術総合研究所を経て現在は東邦大学で研究を行っています。今回紹介する感光性材料は、「実は別の目的で作製した」ものだとか。予想しなかったことを「おや？」「ひょっとしたら？」をバネに研究を続けたことが、新しい材料と、その原理を知ることに結びついたのです。いわば、台本のないドラマや地図のない航海に、好奇心で挑戦した結果ともいえよう。ドキドキ・ワクワクする心がやはり大切なんですね。

新水系フォトポリマー開発

結晶材、ナノ化で〝水溶性〟に

擬似溶解状態を実現 有機溶媒不要に

東邦大

東邦大学・複合物性研究センターの市村國宏理学部特任教授は、非水溶性の増感剤と光酸発生剤を含んだ水系フォトポリマーを開発した。増感剤と光酸発生剤をナノレベルで微結晶化させ、水中で分散、あたかも〝水に溶けたプリ〟をさせることで水中での光硬化反応を可能にした。これによりパターン形成後の未露光部を除去（現像）するだけでなく、ポリマー原液の調製にも水が使える完全水溶性を実現した。また架橋剤同士も架橋することから皮膜強度も優れるとみられる。有機溶媒を使わない環境負荷低減のフォトポリマー材料開発の幅を広げる成果として注目されそうだ。来年一月に発行される米国王立化学会の学術誌「ジャーナル・オブ・マテリアルズ・ケミストリー」に掲載される。

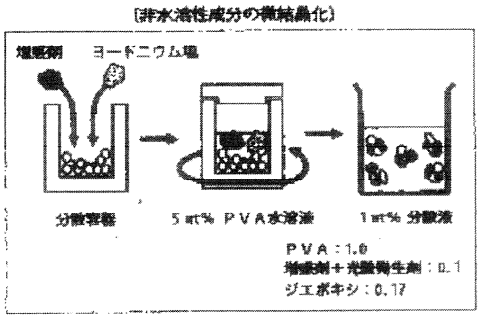

開発したのはポリビニルアルコール（PVA）をベースにした水系フォトポリマー。増感剤は9、10―ジアルコキシアントラセン（DAA）またはイソプロピルチオキサントン（ITX）、光酸発生剤はヨードニウム塩、架橋剤はジエポキシを用いた。水溶性フォトポリマー原液を実現するには反応に関わるすべての成分が水に分子分散、つまり水に溶解している必要がある。しかしPVAとジエポキシは水に可溶だがDAAとITXは不溶、ヨードニウム塩は難溶で、水溶性原液では一連の硬化反応は起こらないとされてきた。

今回、市村教授は非水溶性成分（結晶）の二次粒子径を数百ナノに粉砕することで、ナノ粒子分散でも溶解状態である分子分散のように水中で機能することを発見した。DAAまたはITX、ヨードニウム塩のナノ粒子化はPVAを加え遊星型ミルによって二次粒子が粒径三百―五百ナノ程度にまで粉砕する。これにPVA、ジエポキシを加えて水溶性のポリマー原液に仕上げた。この原液に紫外光（光波長三百五十ナノ）を照射すると増感剤から電子が放出、光酸発生剤が電子を受け取ることで酸を生成する。この酸を触媒として架橋剤とPVAにより硬化（架橋）反応させた。露光後、百二十度C程度で加熱すると架橋は促進する。一方、未露光部（未反応部）は水溶性なので普通の水で洗い流せるので従来のようにPH7アルカリに調整する必要はない。さらに架橋剤同士も架橋するので硬化した皮膜強度も優れる可能性が高い。

非水溶性の増感剤と光酸発生剤が水中で機能したのは一次粒子の直径が電子移動距離より短く、単分子でない凝集体の粒子であっても電子のやり取りが可能だったためと考えられる。今後、一次粒子と二次粒子のサイズの微粒子化、分散性の向上などに取り組み、印刷、エレクトロニクス分野での実用化を視野に入れた環境低負荷のフォトポリマーの開発を目指す。

また今回、ナノ粒子分散によっても水中で分子分散のように振る舞うことが明らかになったことで、非水溶性材料の水系化への新たなアプローチとしてフォトポリマー以外でも応用が進むことも見込まれる。

次世代ＵＶ／ＥＢ硬化技術に向けて

東邦大学理学部特任教授
市村　國宏

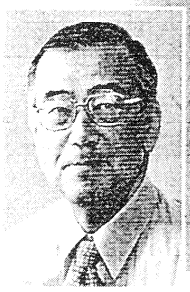

ラドテック研究会設立20周年を記念した講演会が昨秋、東京で開催された。ＵＶ／ＥＢ硬化技術の概況と今後を考える絶好の機会であった。そこで、はじめにその概要を述べ、ついで、ＵＶ／ＥＢ硬化技術の近未来を見直すためにナノテクノロジーとの対比についての考察を試みる。

ラドテック研　創立20周年で講演会

目をみはる中国の成長

西久保忠臣会長の概況報告を受けて、田畑米穂名誉会長から研究会の設立経緯から国内外における活動の展開について豊富な資料に基づく報告がなされた。両氏ともに強調されていることは、多くの学協会が会員数の減少に悩ませられているのに対して、同研究会の会員数はバブル崩壊直後に一時的に若干の減少はあったものの、1986年設立以降減少したことがない、という事実である。1986年から1990年代初頭にかけての急激な会員数増加の時期を経て、バブル崩壊後2002年までは足踏み状態が続いたが、2003年からふたたび着実に増えている。

この背景には、ＵＶ／ＥＢ硬化関連産業の顕著、かつ、着実な成長がある。招待講演者の一人であるＤ．ハルボーン氏（フュージョンＵＶシステム）によれば、1995年から2004年にかけて全世界におけるＵＶ／ＥＢフォーミュレーションの成長率は９％であったが、2004年から2015年でも９％の成長率が見込まれるという。地域別に見ると、北米とヨーロッパで７～８％、アジアでは12％、その他では16％の成長率が予測されている。アジアで特筆すべきは中国の躍進であり、1999年から2004年にかけて素材関連では920％、フォーミュレーションでは205％もの成長を見ている。素材に限らず、フォーミュレーション、インク、塗料などに多くの企業が林立しており、ＵＶ／ＥＢ硬化産業における同国の役割はますます重大となる。

ラドテック研究会設立20周年
記念講演会

加速する機能性重視

こうした世界的な成長路線の中で、応用の内訳に変化が見られる。ＵＶ／ＥＢ硬化技術は、生産性、省エネルギー、環境対応の特徴を活かし、これまで以上にＶＯＣ対策、ＣＯ発生の低減に期待がかかる。各種インク、コーティングなどでは、従来の溶剤系に置き換えるべく、ＵＶ／ＥＢ化の格段の伸張が予測される。その一方で、機能性重視がますます加速されていることに留意したい。わが国でのＵＶ／ＥＢ硬化技術は半分近くがエレクトロニクス用途である点が特徴とされてきたが、欧米でもエレクトロニクス分野に占める割合が増大している。インクジェットインク、さまざまなデジタル製品への取り組みが活発である。ナノテクノロジーとの共存、たとえば、ナノ粒子フィラーやナノ金属を取り込んだＵＶ／ＥＢ製品は、汎用型、高機能型を問わず活躍の場を広げている。

Ｋ．ディートラー氏（チバ・スペシャルティ・ケミカルズ）から光重合開始剤、Ｓ．ディツソン氏（ＢＡＳＦ）からは自動車産業でのＵＶコーティングについての招待講演があった。

個々の応用に特化された光重合開始剤の開発が進められている。典型的な例として、食品包装用やＬＣＤ用カラーフィルターあるいはブラックマトリックス用の光重合開始剤が挙げられる。アミンを触媒あるいは開始剤とするアニオンＵＶ硬化が興味を集めつつあるが、こうした中で、新たな光塩基発生剤についても言及があった。光分解によって３級アミンが発生し、それによってイソシアネートなどの付加反応を触媒することを目的とする。超塩基としての環状アミジンを発生する光塩基発生剤は注目に値する。ただし、光塩基発生剤自体は塩基性物質であり、光分解前後の塩基性の違いを利用する。

熱とのデュアル硬化も

ＵＶ硬化の最大の弱点は複雑な形状で発生する影の部分を硬化できないことだが、光源のロボット化やＵＶと熱とを組み合わせるデュアルキュアによる対応が検討されている。まったく新しいアプローチとしてプラズマ発光による硬化技術が紹介された。装置内で発生するプラズマからの光によりラジカル硬化させることを原理とする。ところで、ＵＶ硬化は自動車産業にすでに各種部材に幅広くとり入れられているが、複雑形状体や影の部分のＵＶコーティングや顔料ＵＶコーティングへの挑戦が続けられている。三次元的にＵＶ照射するために炭酸ガス雰囲気下での硬化システムが開発されている一方で、ウレタンコーティング用のデュアルキュアに適う素材が開発されている。イソシアネート二量体であるアロファネートで連結されたアクリル基とイソシアネート基の双方をもつオリゴマーである。アクリル基でＵＶ硬化させ、イソシアネートとポリオールとで熱硬化を行う。

ＵＶ／ＥＢ硬化技術におけるわが国での強みはエレクトロニクス分野にある。講演会では、林田氏（日立化成工業）、富澤氏（ＪＳＲ）および福口氏（大日本印刷）から多彩な技術紹介がなされた。ＵＶ／ＥＢ硬化を戦略的な技術と位置づけて永年にわたって展開されている成果であり、この技術分野における勝ち組という印象を強く受けた。これら企業に限らず、素材、フォーミュレーション、線源、装置関連に多くの勝ち組があり、それぞれが日々努力を重ねていることを心強く思う。

ナノテクとの対比・考察

ところで、最近、「なぜ、ナノテクは行き詰ったのか？」という記事が目に入り、驚いた（週刊エコノミスト臨時増刊２／12号、104ページ）。クリントン政権が国家ナノテクノロジー戦略を策定したのが2000年であり、2001年にわが国で国を挙げての施策が打ち出されたことは記憶に新しい。行き詰ったとする根拠は、2010年のナノテク関連市場規模の当初予測値が一桁ほど下方修正されていることにあるようだが、学術分野でいえば、アメリカ化学会がＮａｎｏ　Ｌｅｔｔｅｒを発刊したのが2001年であるし、Ｎａｔｕｒｅの姉妹誌としてＮａｔｕｒｅ　Ｎａｎｏｔｅｃｈｎｏｌｏｇｙ誌がスタートしたのは昨年10月のことである。ナノを冠する用語が溢れる以前にすでに、多くのナノサイズの超薄膜や超微粒子からなるナノ製品などが世に出ている事実もあり、フォトポリマーとともにナノ材料の基礎研究の片隅に身を置く筆者にとって、すっきりしない指摘であった。おそらく、フラグシップ型プロジェクトと銘打った次世代半導体、大容量情報ストレジおよびネットワークデバイス技術への直接的な波及効果が今ひとつ、ということなのだろう。

波及効果高いＬＣＤ関連

ここで唐突にナノテクノロジーをあえて取り上げたのは、基幹的産業技術として定着したＥＢ／ＵＶ技術と対比させることは一興だと思うからである。ＥＢ／ＵＶ技術の市場規模のデータはＥＢ／ＵＶ製品の量に基づく場合が多い。ＥＢ／ＵＶ製品を素材もしくは部材として組み上げた最終製品の市場規模に換算すると、大きな数字となる。一例として、ＵＶ製品としてのナノ顔料分散型フォトポリマーを取り上げる。ちなみに、これは顔料の光散乱を極限まで抑制した先駆的なナノテク製品にほかならないが、筆者は20年以上も前に開発にかかわった経緯があり、とりわけ関心が深い。2005年でいわゆるカラーレジストは600億円弱、それを用いるカラーフィルターは3000億円に達している。波及効果として最終製品であるＬＣＤの市場まで広げれば、その規模は膨大となる。ＬＣＤはさらに多くのＵＶ製品から構成されている。今後は、光分子配向とＵＶ硬化の融合やＵＶ／ＥＢ硬化による各種部材のＲｏｌｌ－ｔｏ－ｒｏｌｌ製造プロセスへと進展するだろう。また、さまざまなフォトレジストもＵＶ製品に属するから、半導体技術の規模を考慮すれば、これら先導的産業への高機能性ＵＶ／ＥＢ製品の貢献はきわめて大きい。

ナノテクノロジーには、ＩＴ、バイオ、エネルギー・環境、材料などにおけるブレークスルーが期待されている。その根幹をなすのがナノレベルで構造や組成配合が制御された材料技術とその製造プロセスであり、そのためにナノレベルでの計測やシミュレーションが不可欠となる。ありふれた既存物質を用いてナノレベルでの構造を観察し、発現する諸物性を発見して高機能性材料に仕立て直すことは研究者としてこれほど痛快なことはない。しかし、こうした基礎研究の成果が製品化に円滑に結びつくとは限らない。一般的に、ナノレベルで観察され評価される材料の領域は限定的であり、キログラムあるいはトン単位の材料やそれを用いるデバイスすべての部分において、精緻に構造制御されているとは限らないからである。ナノテク関連の学術論文でも美しいグラフィックスによってナノ構造が表示されることが多いが、筆者は実像と峻別することを心がけている。だからこそ、基礎的な研究の積み重ねが必須であり、それなりの時間を要する。

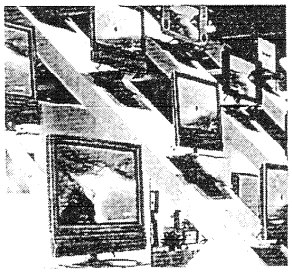

根源的な研究開発重要

こうして考察すると、ＥＢ／ＵＶ硬化技術はナノテクノロジーと対照的な様相を示している気がする。ナノテクノロジーでは基礎研究の重要性が認知される一方で、以前からナノテク製品が世に出ているとはいえ、産業技術への展開にもどかしさがある。ＥＢ／ＵＶ技術は即効的であり貢献に実用範囲を拡大しているが、改良研究によりある程度の対応が可能なためか、とりわけ官学研究機関での基礎的な取り組みがわが国では非常に脆弱である。ナノテクを標榜する研究者の数と比較すればよい。素材関連に限定した課題の数例を挙げれば、ラジカル種や強酸分子の硬化膜中での挙動は未開拓な研究領域であるし、ラジカル重合における硬化収縮や酸素阻害の根源的な解決は図られていない。フッ素系ＵＶカチオン重合開始剤に代わる高効率開始剤や硬化後における強酸の処理に関しては無策のままである。エポキシやウレタン硬化に新たな局面を拓くと期待される光塩基発生剤には、上述のように新たな展開が見受けられるが、高効率開始能を持つ中性の光塩基発生剤が望まれる。厚膜や影の部分の硬化への挑戦は上述の例も含めていくつかなされているが、いまだ不十分である。

ＥＢ／ＵＶ硬化は成熟した技術ではない。学問的な裏づけへの努力も乏しい。今後も着実に成長することはいうまでもないが、ナノテクノロジーとの融合をも含めた可能性をさらに引き出すためには、以上のような根源的な研究開発への取り組みが必要だと強く思う。